NEW EVIDENCE FOR COMPLEX MOSASAUR PALEOBIOLOGY: OXYGEN ISOTOPES IN ENAMEL REVEAL HABITAT VARIATION OF *CLIDASTES* FROM THE MOOREVILLE CHALK, ALABAMA

by

LEAH TRAVIS TAYLOR

REBECCA TOTTEN MINZONI, COMMITTEE CHAIR
W. JOE LAMBERT
THOMAS TOBIN
CELINA A. SUAREZ

A THESIS

Submitted in partial fulfillment of the requirements
for the degree of Master of Science
in the Department of Geological Sciences
in the Graduate School of
The University of Alabama

TUSCALOOSA, ALABAMA

2019

ABSTRACT

The Late Cretaceous Mississippi Embayment includes some of the most complete, well-preserved mosasaur specimens in the world. Here I investigate the paleobiology of these extinct swimming lizards through schlerochronological analysis of fossil teeth with unparalleled temporal resolution. By analyzing the oxygen isotope composition of enamel phosphate in eight consecutive, fully erupted teeth, I reconstruct the ecological niche of a *Clidastes propython* individual from the Mooreville Chalk in Pickens County, Alabama. The isotopic record is then compared with the previously studied *Platecarpus ictericus* mosasaurs from the time-equivalent Kansas Niobrara Chalk of the Western Interior Seaway.

Phosphate oxygen isotope records from all eight teeth in the *C. propython* specimen correlate well and are spliced to build a longer record of water composition change. The spliced isotopic record is characterized by two primary features: 1.) well-correlated, semi-regular negative spikes in $\delta^{18}O$ that have a 12 to 20 day recurrence and are up to ~4.0‰ amplitude, and 2.) a long-term decrease in $\delta^{18}O$ from ~21.5‰ to ~20.0‰ (‰ V-SMOW), followed by a gradual increase to ~22.0‰ and a final decrease to ~20.0‰. The short-term excursions in $\delta^{18}O$ indicate rapidly changing water habitats for the mosasaur, possibly resulting from incursion into freshwater sources with low $\delta^{18}O$ composition. Semi-regular incursion of the *C. propython* individual into freshwater suggests that mosasaurs had osmoregulatory function similar to those of their living relatives, sea snakes, who must drink freshwater periodically. The long-term trend in $\delta^{18}O$ further suggests that the *C. propython* individual may have migrated from open ocean water into the shallow, evaporative, ^{18}O-enriched environments of the Mississippi Embayment.

The mean $\delta^{18}O$ value of the Alabama *C. propython* is ~3.7‰ higher than that of the Kansas *P. ictericus*. This difference is likely due to the varying isotopic composition of the open, central Western Interior Seaway vs. the evaporative, lower latitude Mississippi Embayment. An important similarity between the *P. ictericus* and the *C. propython* is that they both exibit semi-regular, negative excursions in $\delta^{18}O$, further implicating the freshwater incursions to be the result of a biological requirement spanning multiple, if not all, mosasaur genera.

DEDICATION

This thesis is dedicated to my father, Steve Travis, for always believing in me and inspiring me to work hard and follow my dreams, and to my mother, Christy Travis, for her constant support and love. I would also like to dedicate this to my loving husband, Zak Taylor, who stood by my side throughout this entire process and never stopped encouraging me.

LIST OF ABBREVIATIONS AND SYMBOLS

ºC	degrees Celsius
$\delta^{18}O$	Delta Notation $\delta^{18}O = \left[\left({}^{18}O/{}^{16}O_{sample} - {}^{18}O/{}^{16}O_{standard}\right) \div \left({}^{18}O/{}^{16}O_{standard}\right)\right] \times 1000$
%	percent
‰	per mil
µg	micrograms
σ	standard deviation
cm	centimeters
GOM	Gulf of Mexico
IRMS	Isotope ratio mass spectrometer
km	kilometers
m	meters
Ma	Million Years Before Present
ME	Mississippi Embayment
mm	millimeters
TC/EA	High-Temperature Conversion Elemental Analyzer

V-SMOW	Vienna Standard Mean Ocean Water
WIS	Western Interior Seaway

ACKNOWLEDGEMENTS

Foremost, I would like to thank my advisor, Dr. Rebecca Totten Minzoni, whose guidance and support enabled me to complete this thesis and grow as a scientist. Her passion for geology and brilliant mentoring skills gave me to confidence to succeed and pursue my academic goals. I am also indebted to Dr. Celina Suarez for her advice and instruction throughout my entire project, but in particular for her help with the silver phosphate method and for allowing me to work in the UASIL (University of Arkansas Stable Isotope Laboratory). I also appreciate the advice and knowledge from my internal committee members, Dr. Tom Tobin for his comprehensive scientific conversations and Dr. Joe Lambert for his unwavering support through the ASIL (Alabama Stable Isotope Laboratory). I am thankful to Dr. Dana Ehret for his assistance in obtaining the analyzed fossil specimen and his extensive paleontological knowledge and advice, as well as to Dr. Lynn Harrell for his mosasaur expertise. Dr. Alberto Pérez-Huerta provided much support and knowledge during the SEM (Scanning Electron Microscope) analysis of my samples. I am also appreciative of the excellent guidance and support given by Dr. Fred Andrus during my time at UA. Finally, I am extremely grateful for all the assistance from fellow students along the way. Christine Bassett provided wonderful advice and tremendous support on the micromill and thin sectioning methods. Rachel Mohr and Rebecca Greenberg contributed micromill expertise and centrifuge assistance, respectively, as well as witty geology puns. Kaydee West and Carmen Atkins provided invaluable presentation advice and encouragement. Jamekia Durrough-Pritchard supplied constructive biomineral conversations. Taylor Woods and Travis Sizemore contributed appreciated thesis-writing advice, and Adlai Fonseca, Lauren

Parker, Victoria Fitzgerald, Kyle Olsen, Lucas Nibert, Joel Sobrado, Asmara Lehrmann, and Danielle Secor have been amazing scientists to share a lab with the past two years.

CONTENTS

LIST OF TABLES

LIST OF FIGURES

INTRODUCTION

Mosasaurs were prolific swimming reptiles of the Late Cretaceous seas and went extinct at 66 Ma due to the K-Pg mass extinction, along with numerous other abundant megafauna, such as dinosaurs (e.g., Macleod et al., 1997; Brusatte et al., 2014; Longrich et al., 2012). During the last 25 million years of the Cretaceous, mosasaurs rapidly diversified into markedly successful marine predators, filling top predator niches by the end of the Cretaceous (Schulp, 2005). They were globally distributed, with a great abundance in the Western Interior Seaway (WIS) and Mississippi Embayment (ME) of North America (Fig. 1; Ross, 2009; Harrell and Pérez-Huerta, 2015; Russell 1967; Martin et al., 2002). Several genera of mosasaurs are found in the North American provinces, with an abundance of *Clidastes spp.* in the ME and *Platecarpus spp.* in the WIS.

Teeth and bones of mosasaurs are well-preserved in the WIS and ME chalk deposits and present an opportunity to determine isotopic composition of original fossil material. Fossil tooth enamel is targeted due to resistance to alteration; the phosphate oxygen is tightly bound in the phosphate anion, making it a useful paleoenvironmental proxy (Kohn and Cerling, 2002). The *Clidastes spp.* mosasaurs have conical, posteriorly recurved teeth (Russell, 1967), homodont dentition (Massare, 1987), and inferred daily incremental growth lines, with wider growth bands representing ~11-13 days of enamel accretion, based on incremental line width measurements and growth line counts (Gren and Lindgren, 2013).

Phosphate $\delta^{18}O$ is strongly influenced by the $\delta^{18}O$ of the body water. In addition, deviation can occur through fractionation that is caused by internal temperature fluctuations (Clementz and Koch, 2001). In fully marine organisms incapable of travelling onto land,

$\delta^{18}O_{bodywater}$ of the organism should be equivalent to the $\delta^{18}O_{seawater}$ (Newsome et al., 2010; Koch 2007; Clementz and Koch, 2001). Although there are no precise modern analogues for mosasaurs, they were aquatic-bound swimming lizards; therefore, modern fully marine organisms incapable of traveling on land may provide the best comparison. Studies on modern fully marine organisms, such as cetaceans and pinnipeds, indicate that their body water isotopic ratio is comparable to the isotopic ratio of the water that they inhabit (Clementz and Koch, 2001; Yoshida and Miyazaki, 1991). When tooth enamel forms, the biogenetic phosphate derives its oxygen isotope ratios from the water present in the body of the organism (Straight et al., 2004). Therefore, if $\delta^{18}O_{bodywater}$ is in equilibrium with $\delta^{18}O_{seawater}$, and $\delta^{18}O_{phosphate}$ is derived from $\delta^{18}O_{bodywater}$, it follows that changes in the $\delta^{18}O_{phosphate}$ should directly indicate changes in the isotopic composition of the water that the mosasaur was inhabiting.

One additional factor that may affect $\delta^{18}O_{bodywater}$ and thus $\delta^{18}O_{phosphate}$ is the thermoregulation system of the organism. If the body temperature of an organism fluctuates daily based on external temperature changes, then the organism has ectothermic thermoregulation; however, if the organism produces body heat and maintains a stable internal body temperature, then it has endothermic thermoregulation (Feduccia, 1972). In endothermic marine organisms, the isotopic ratio in the $\delta^{18}O_{bodywater}$ is dominated solely by the $\delta^{18}O_{seawater}$ due to a constant internal temperature and thus a constant fractionation (Clementz and Koch, 2001; Longinelli, 1984; Luz et al., 1984). Previous research using oxygen isotopes in fossil bioapatite indicates endothermic thermoregulation in Late Cretaceous mosasaurs (Harrell et al., 2016). Mosasaur fossils have been found on every continent, including Antarctica (Russell 1967; Martin et al., 2002; Harrell and Pérez-Huerta, 2015; Ross, 2009); as ectothermic reptiles in polar regions are rare even in greenhouse climates (de la Fueta et al., 2010), this further supports the adaption of

endothermy in mosasaurs. Thus, the oxygen isotope ratios in mosasaur teeth are likely derived from the water composition that the mosasaur inhabited, and not internal body temperature fluctuations. The oxygen isotope ratios preserved during the sequential growth of a mosasaur's tooth, therefore, record the $\delta^{18}O$ value of the water in which the mosasaur occupied at the time of enamel precipitation. The $\delta^{18}O$ value of the surrounding environmental water is a marker of salinity and temperature due to fractionation through hydrologic processes such as evaporation and precipitation, and tracks with differences in water sources. The $\delta^{18}O$ composition in the biogenetic phosphate serves as a proxy for the environmental conditions where the mosasaur lived and how frequently it migrated based on incremental changes in these isotopic ratios.

If mosasaurs were ectothermic, however, it may not have affected their $\delta^{18}O_{bodywater}$ if the water they inhabited remained at fairly constant temperatures. For example, some modern ectotherms, such as certain tropical fish, are technically homeotherms (maintain constant internal body temperature) rather than poikilotherms (experience a wide range of internal body temperatures) because they inhabit an environment with invariable ambient temperatures, thus their internal temperature remains constant (Madden et al., 2004; Feduccia, 1972). The Late Cretaceous was a warm, greenhouse world (Steuber et al., 2005; Coulson et al., 2011), so it may have been possible for an ectothermic mosasaur to have a narrow range of body temperature. Still, to account for any possibility that mosasaurs were actually ectothermic or only partially endothermic and poikilotherms, body temperature equations in Lécuyer et al. (2013) will be utilized to explore the expected impact of daily internal temperature fluctuations that an ectothermic organism would experience to constrain the additional variable of temperature-dependent fractionation.

Phosphate oxygen isotopes in tooth enamel from Kansas *P. ictericus* specimens (Fig. 1)

were used to compare juvenile versus adult migration habits; the results suggest evidence for migratory behavior and freshwater incursion in the WIS (Totten, 2009). The paleoecology and migration habits of mosasaurs from the southeastern U.S. have yet to be investigated using oxygen isotopes, however. Presented here is a paleoecological interpretation based on oxygen isotope data generated by using isotopic methods (O'Neil et al., 1994; Straight et al., 2004; Totten 2009; Kohn and Cerling, 2002; Harrell et al., 2016) on a *C. propython* specimen from the southeastern U.S. in the Late Cretaceous ME (Fig. 1). Oxygen isotope composition of phosphate in fossil tooth enamel is analyzed to interpret the water salinity and temperature in which the mosasaur individual lived. A muli-month time series based on an inferred time determination of mosasaur growth lines (Gren and Lingren, 2013) is constructed through correlation of isotopic records from fossil teeth in series to reconstruct water composition change and paleomigration of the *C. propython* specimen. The Alabama *C. propython* $\delta^{18}O$ record is compared with the Kansas *P. ictericus* $\delta^{18}O$ record to investigate the biology of these extinct predators and further compare the paleomigration habits of mosasaurs in the ME to those of the WIS.

Significance

In the face of ongoing climate change, there are concerns of how large marine organisms and their seasonally associated behavior, namely migration and reproduction, will be impacted by rising water temperatures and sea level. In addition, sea snakes, a living relative of mosasaurs, are currently being threatened by climate change, with declining populations and recent extinctions (Lillywhite et al., 2008). By studying mosasaurs, who potentially had a similar osmoregulatory system to sea snakes, my research may help inform these discussions by contributing perspectives on the migratory behavior of extinct marine reptiles that lived during the warm greenhouse climates of the Late Cretaceous.

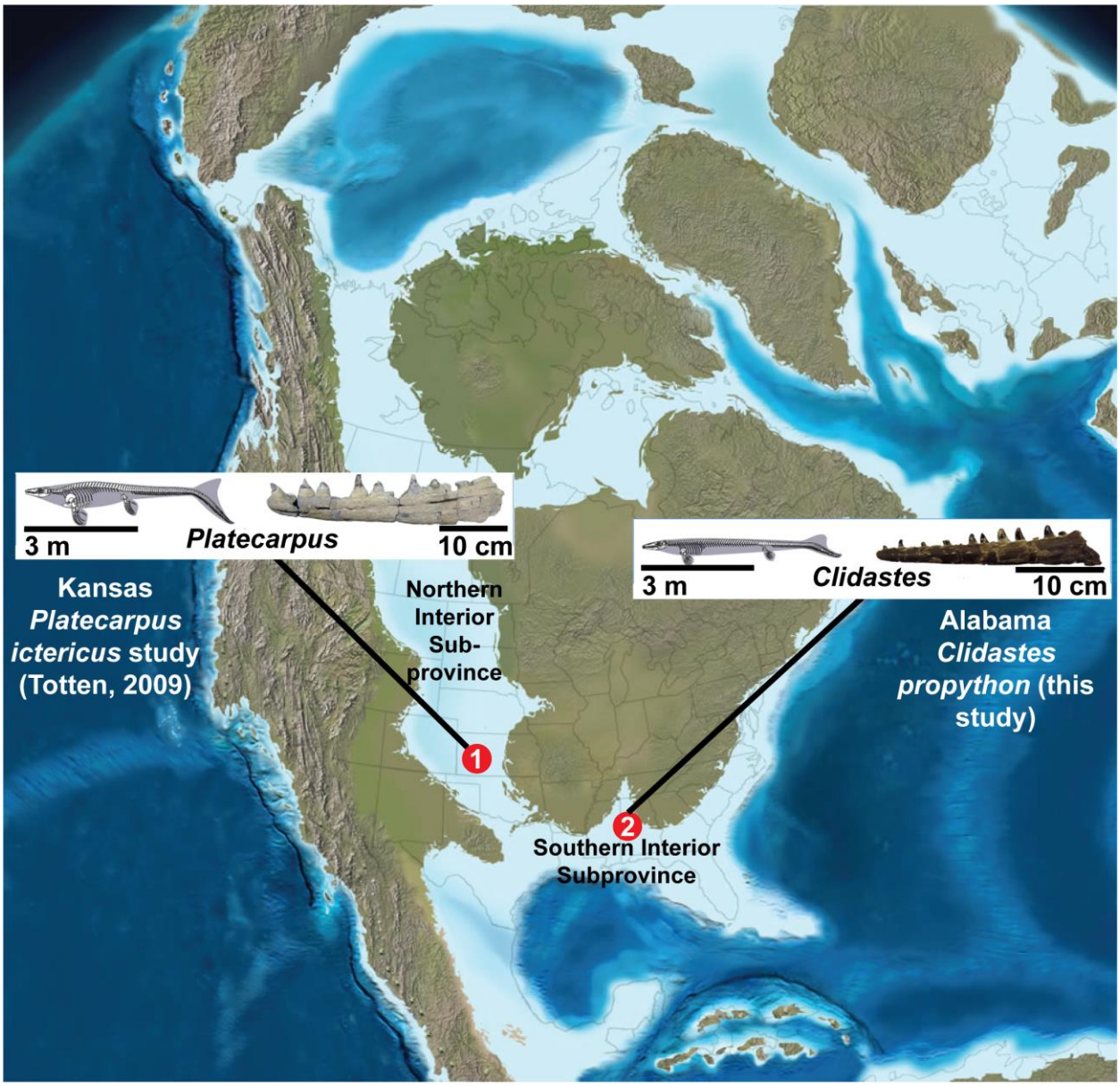

Figure 1: Cretaceous Paleogeography with faunal provinces of the Cretaceous Western Interior Seaway. 1.) Kansas *Platecarpus ictericus* study location (Totten, 2009), and 2.) Alabama *Clidastes propython* study location (image modified after Blakey, 2017; Nicholls and Russell, 1990; Totten, 2009; Harrell et al., 2016).

BACKGROUND

Mosasaur Paleobiology

Mosasaurs were marine lizards that were exceptionally specialized to their aquatic habitats. They are estimated to have lived up to ~30 years old, based on LAGs (lines of arrested growth) in mosasaur humeri (Pellegrini, 1998), and they had a wide range of dietary preferences, some of which include bony fish, ammonites, belemnites, cephalopods, sharks, and marine reptiles, including turtles and other mosasaurs (Massare, 1987; Ross, 2009; Russell, 1967). Mosasaurs exhibit a broad spectrum of tooth morphologies among species due to their extensive dietary range (Fig. 2; Massare, 1987; Ross, 2009). *Clidastes* mosasaurs have tooth morphologies designed for cutting and slender jaws adapted to rapid biting, suggesting they were likely generalist ambush predators, eating everything from bony fish to sea birds, according to their body size (Ross, 2009; Russell, 1967). In addition to their broad dietary range, it is possible that mosasaurs competed with each other territorially and during mating, like modern lizards (Lingham-Soliar, 2004; Everhart, 2008). Evidence from bites and fractures in mosasaurs suggest intraspecific agonistic behavior (Bell and Martin, 1995; Schulp et al., 2004; Rothschild and Martin, 2006, Lingham-Soliar, 2004; Everhart, 2008). Mosasaur fossils also show evidence for viviparity (Caldwell and Lee, 2001; Blackburn and Sidor, 2014; Field et al., 2015). The development of live birth and a broad dietary range were important adaptions for fully marine lifestyles.

Due to the complex biology of these extinct swimming squamate lizards, their paleoecology remains uncertain. In particular, the paleoecological habits of one of the smaller

mosasaur genera called *Clidastes* is unclear. Some studies (Field et al., 2015; Kiernan, 2002) suggest based on fossil evidence that *Clidastes* was a pelagic genus, while in contrast Russell (1967) proposed based in part on Kansas fossil discoveries that *Clidastes spp.* inhabited near-shore water. Using rare earth elements, recent research indicates that *Clidastes* may have had wider habitat preferences ranging from middle to inner shelf environments; however, the results were inconclusive (Harrell and Pérez-Huerta, 2015). Another study (Lindgren and Siverson, 2004) found that within the Kristianstad Basin area, Sweden, *Clidastes* occurs in shallow water deposits, and proposed that *Clidastes spp.* were generally near-shore organisms. Lindgren and Siverson (2004) further suggested that *Clidastes spp.* may have exhibited long-range migratory behavior, migrating from the ME and WIS to parts of Europe. Totten (2009) investigated the paleoecology of Kansas mosasaurs using phosphate oxygen isotopes in fossil tooth enamel from *Platecarpus ictericus* specimens; the results suggested evidence for migratory behavior and freshwater incursion. The Kansas *P. ictericus* study serves as the foundation for this thesis, in which I conduct the first schlerochronological analysis on mosasaurs from the southeastern U.S. (Fig. 1).

Geologic Background

During the Cretaceous Period, much of the current southeastern U.S. was inundated by a shallow sea, which connected to an epeiric seaway known as the Western Interior Seaway (WIS). This seaway is divided into two main faunal provinces: Northern Interior Subprovince, which had lower faunal diversity and a mild climate, and Southern Interior Subprovince, which had a subtropical climate and higher faunal diversity (Fig. 1; Nicholls et al., 1990). Although *Clidastes spp.* and *Platecarpus spp.* inhabited both subprovinces, the mosasaur genus *Clidastes* dominated the waters in what is now the southeastern U.S., while the Northern Interior Subprovince of the

WIS was dominated by the genus *Platecarpus*; therefore, the two genera likely exhibited niche differentiation (Figs. 1 and 3; Nicholls et al., 1990).

The *Clidastes propython* specimen (ALMNH 3837) for this study was collected from the upper Santonian to lower Campanian Mooreville Chalk Formation in Pickens County, Alabama. The Mooreville Chalk Formation was deposited in an inner or middle shelf environment and ranges from 107 to 122 m in stratigraphic thickness (Liu, 2009). Vertebrate fossil remains in the Mooreville Chalk are exceptionally well-preserved, both chemically and physically, due in large part to minimal diagenetic alteration in the impermeable chalk units (Liu, 2009; Harrell et al., 2016). The *Platecarpus ictericus* specimens studied by Totten (2009), which will be compared with the *Clidastes propython* of this study, were collected from the middle Santonian to lower Campanian Smokey Hill Chalk Member of the Upper Cretaceous Niobrara Chalk in western Kansas. The Smokey Hill Chalk Member averages 182 m in stratigraphic thickness and was deposited in a calm, shallow sea (Everhart, 2001).

Paleoceanographic setting and isotopic relationships

Using a Late Cretaceous temperature gradient of 0.4°C per degree of latitude (Amiot et al., 2004), the temperature difference would have been ~2.8°C between the habitats of the ME (present-day Alabama) and the WIS (present-day Kansas). This is a worldwide temperature gradient being employed across a small latitude range, however, and therefore is applied with caution. Recent research using isotopic data from turtle and fish bone indicates a temperature difference of 3 to 4°C between the two subprovinces (Coulson et al., 2011), closely corroborating with the calculated temperature difference using the worldwide temperature gradient. Studies have further suggested temperature zonation that caused biogeographical subdivisions in the seaway (Nicholls et al., 1990). In the WIS, increased contribution of

freshwater and salinity-driven stratification is suggested from clumped isotopes and oxygen isotopes of mollusk shells (Petersen et al., 2016; Dettman and Lohman, 2000). Moreover, elevated salinity of surface waters in the ancestral Gulf of Mexico (GOM) during the Cretaceous has been proposed (Woo et al., 1992; Pagani and Arthur, 1998). Therefore, with these regional temperature and salinity variations, the isotopic signal between the Alabama *C. propython* and Kansas *P. ictericus* specimens should be pronounced enough to characterize the different paleoenvironments. Freshwater-influenced coastal systems (i.e., estuaries) are characterized by a pronounced lower $\delta^{18}O$ than open marine systems of the ancestral GOM and WIS, while more evaporative, saline systems, such as shallow lagoons and restricted basins, are characterized by a higher $\delta^{18}O$ (Fig. 4). The $\delta^{18}O$ composition in the biogenetic phosphate serves as a proxy for the oceanographic settings and environmental conditions where the mosasaurs lived and how frequently it migrated based on incremental changes in these isotopic ratios (Fig. 4; Zazzo, 2004).

Mosasaur Dentition: incremental growth lines

Mosasaur teeth have incremental *lines of von Ebner* that represent daily enamel accretion, and wider bands called *Andresen lines* representing ~11-13 days of enamel accretion (Gren and Lindgren, 2013). The time determination of von Ebner and Andresen lines was calculated based on counted lines in mosasaur tooth thin sections that correlate well with those observed in modern mammals and reptiles, as well as fossil dinosaur teeth (Gren and Lindgren, 2013; Erickson, 1996). Based on incremental line width measurements and growth line counts, each tooth possibly took up to ~8-16 months to form (Gren and Lindgren, 2013). Based on observations of the closest living relative of mosasaurs, the monitor lizard *Varanus komodoensis*, and counts of the daily surficial enamel growth lines, however, each tooth may have formed in as

little as ~3 months (Pellegrini, 1998; Totten, 2009). Surficial growth line counts performed on the sampled *Clidastes* teeth indicate that they took an average of 3 to 4 months to grow (see Appendix B). Mosasaur teeth grow in a staggered replacement pattern (Fig. 5; Caldwell, 2006). The growth lines of the mosasaur teeth can be sampled incrementally to produce a time-series of $\delta^{18}O$ composition, and thus past water composition. The records of several teeth in a mosasaur jaw can be spliced and correlated to produce a long-term, multi-month isotopic record.

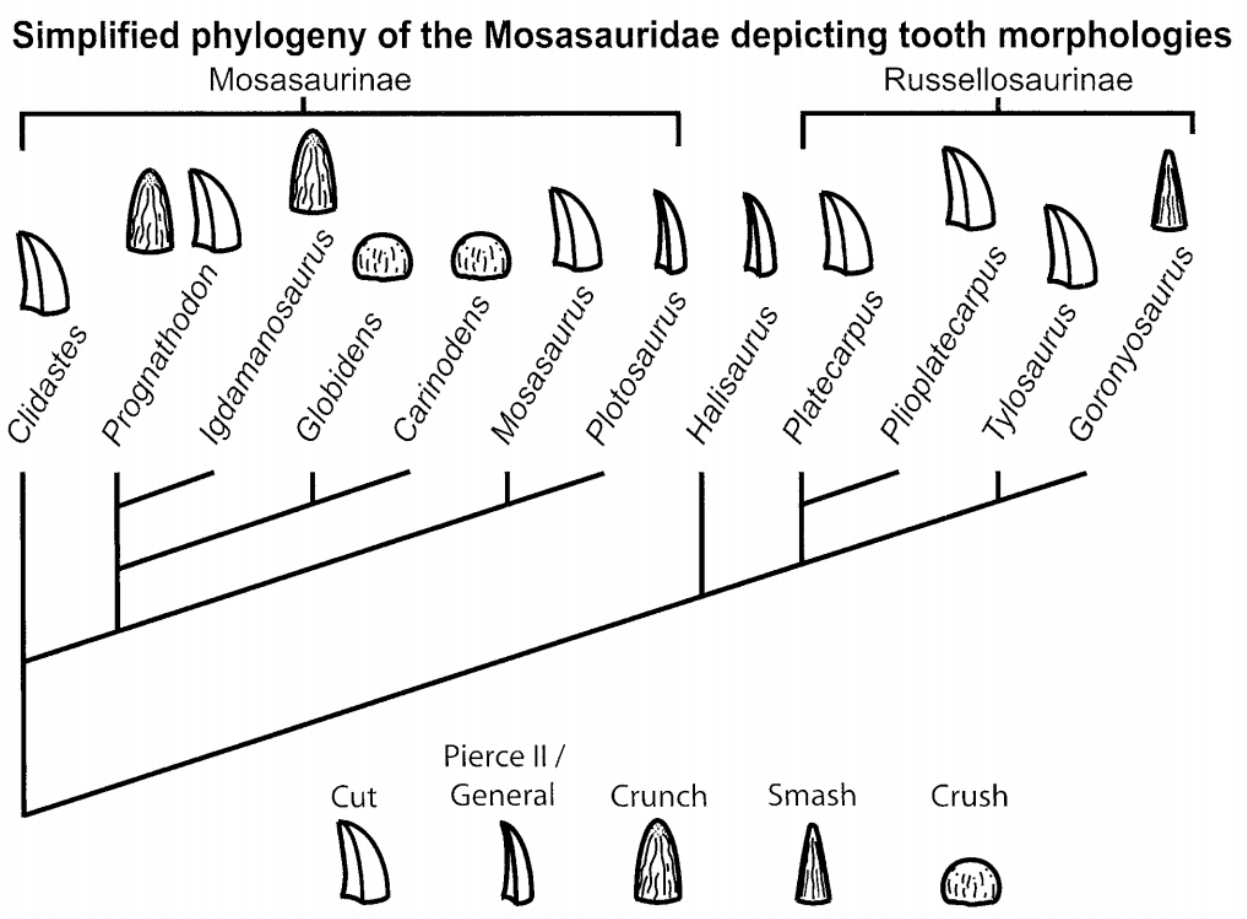

Figure 2: Mosasaur tooth morphologies. The diverse variations are related to widely ranging dietary preferences (Ross, 2009).

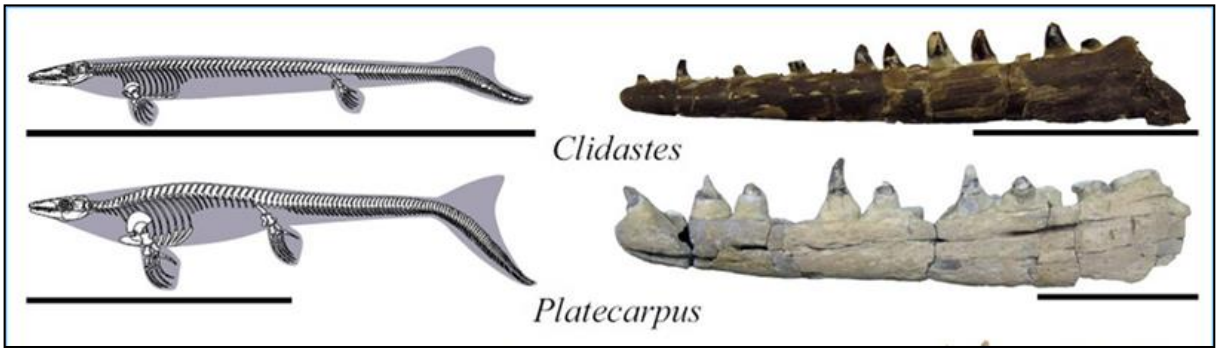

Figure 3: Mosasaur genera *Clidastes* and *Platecarpus*. Scale bars represent 3 m (left) and 10 cm (right) (image modified after Harrell et al., 2016).

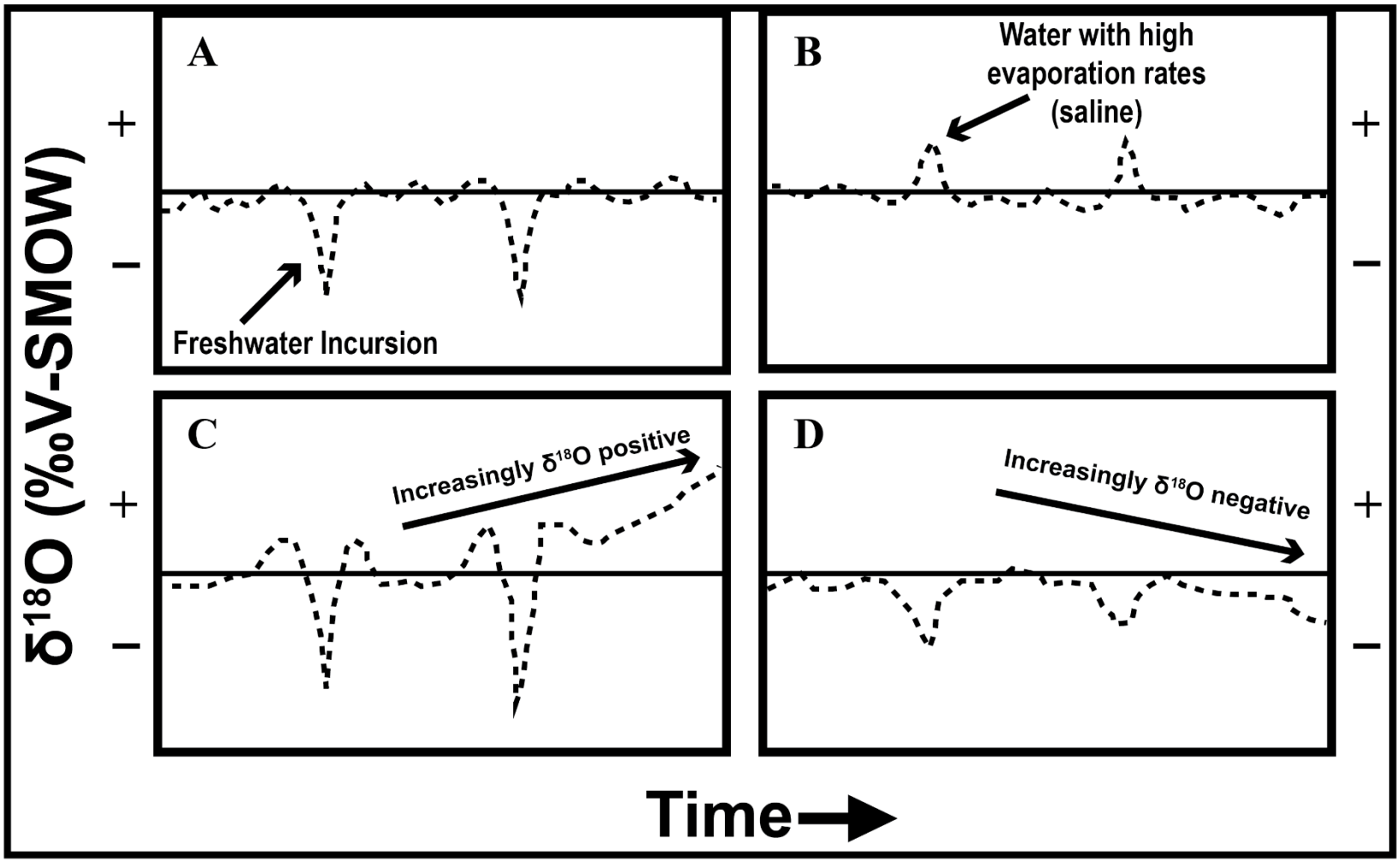

Figure 4: Expected $\delta^{18}O$ results. Predicted $\delta^{18}O$ variation with time if the mosasaur was (A) frequenting freshwater environments with ^{18}O-depleted water, (B) frequenting saline environments with ^{18}O-enriched water, (C) Migrating into increasingly $\delta^{18}O$ positive water while frequenting freshwater environments with ^{18}O-depleted water, and (D) Migrating into increasingly $\delta^{18}O$ negative water while frequenting freshwater environments with ^{18}O-depleted water (image modified after Totten, 2009).

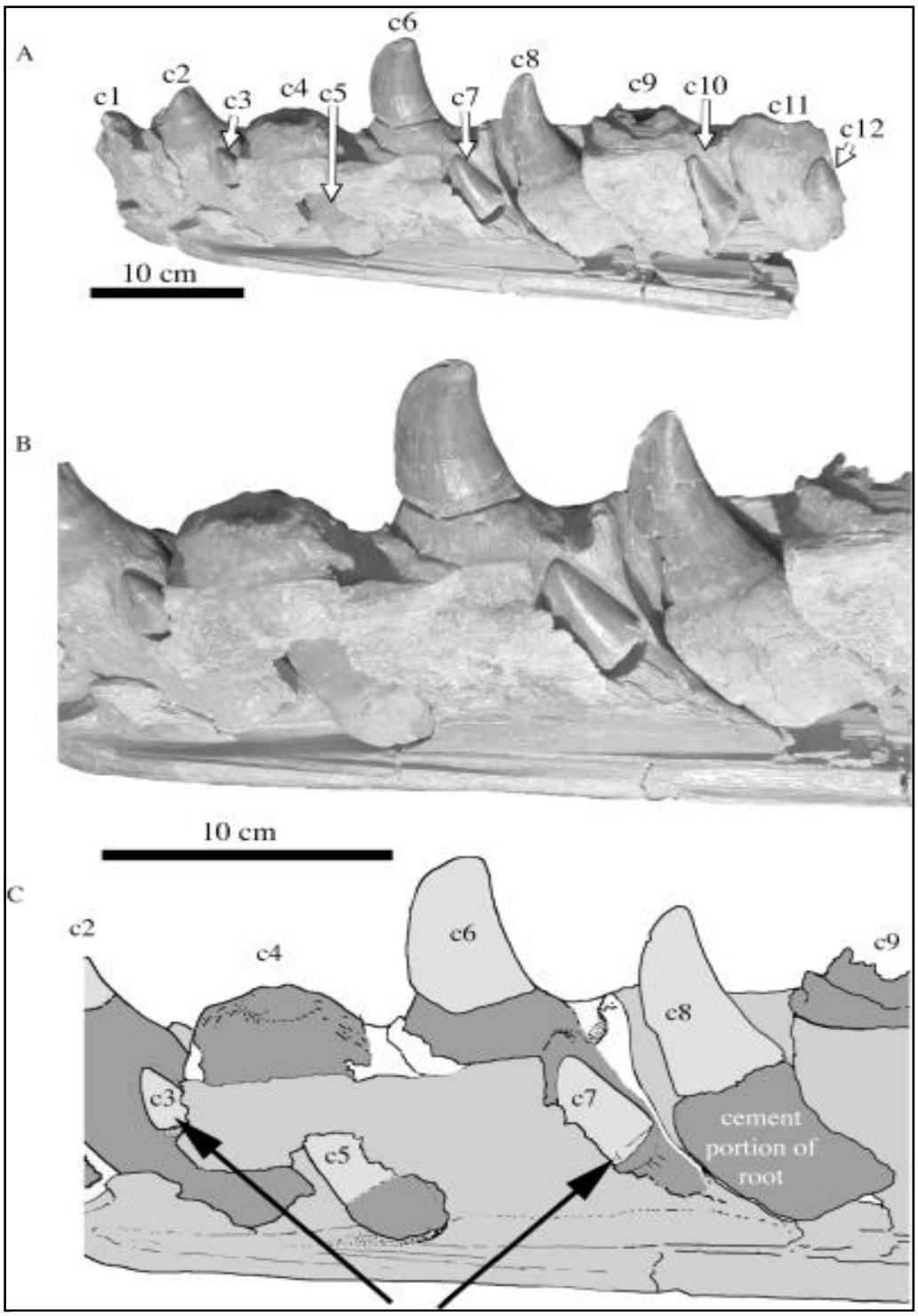

Figure 5: Staggered replacement of mosasaur teeth. Numbers are sequential; c = tooth crown (Caldwell, 2006).

METHODS

Here I analyze a *Clidastes propython* upper right maxilla containing eight complete posterior teeth and five replacement teeth (Fig. 6). The maxilla section was 3D scanned in the University of Alabama 3D prototyping laboratory to print a 3D model of the jaw, as well as image changes in the curvature of the teeth that serve as an indicator of growth increments (Fig. 7). The 3D prototyping lab used a Stratasys Dimension SST 1200es commercial grade 3D printer with a layer thickness of 0.254 mm. Externally observed growth lines within each tooth of the specimen were finely sampled using a tungsten carbide 0.25 mm bit micromill in the Alabama Stable Isotope Laboratory (ASIL). The teeth were drilled at a shallow depth (~150 μm) to target the enamel layer and avoid drilling the internal dentine, which is porous and susceptible to alteration (Kohn and Cerling, 2002).

Fossil preservation was evaluated by imaging the microstructure of the enamel crystals in an isolated tooth from the same *C. propython* specimen, following Chinsamy et al. (2012). The potential presence of secondary recrystallization and quality of preserved bundles of bioapatite crystals were assessed to verify preservation. No recrystallization was observed, and throughout the enamel layer bundles containing bioapatite crystals were apparent, indicating exceptional preservation. Scanning Electron Micrograph (SEM) results show that the original enamel is prismatic in structure and is not diagenetically altered; in fact, the specimen is so well-preserved that the porous dentine is also unaltered (Fig. 8). A piece of the enamel layer from one of the sampled teeth within the jaw was also imaged with the SEM and further confirms exceptional preservation of the study specimen (Fig. 9). An analogous model of SEM enamel microstructure

examination was employed to assess diagenesis of Upper Cretaceous shark teeth from Alabama; similar exceptional preservation of fossil enamel was found, including a prismatic structure that compared well to modern shark enamel microstructure, confirming the integrity of the specimen (Harrell et al., 2016). Although there are no living mosasaurs to directly compare, SEM microstructure analysis of a modern Iguana enamel reveals similar microstructure as the preserved *Clidastes* mosasaur in this study (Wang et al., 2006).

Between 45 and 50 samples, each weighing 300 to 500 µg, were drilled using a micromill from all eight erupted teeth in the *C. propython* jaw, totaling 340 samples for $\delta^{18}O$ analysis. The upper maxilla section containing the eight teeth was photographed again post-drilling to compare the sampling lines to the growth lines, and the sampling lines were viewed under a microscope to ensure the lines were drilled within the enamel. The samples were then prepared in the ASIL to isolate the enamel phosphate by using the silver phosphate method to obtain $Ag_3PO_4(s)$ from the $Ca_5(PO_4)_3OH$ (Fig. 10; method modified after O'Neil et al., 1994; Zazzo et al., 2004; and Vennemann et al., 2002). Precipitated Ag_3PO_4 crystals were analyzed at the University of Arkansas Stable Isotope Laboratory (UASIL) using a TC/EA (High-Temperature Conversion Elemental Analyzer). Ag_3PO_4 crystals reacted with graphite at 1400°C to form CO gas and the $\delta^{18}O$ composition was measured from the CO using a Thermo Finnigan Delta Plus XL gas chromatograph Isotope Ratio Mass Spectrometer (IRMS) (Fig. 10). The external precision is ±0.3‰ and was assessed with internal standards. UASIL used the following internal standards: ANU Sucrose, Alpha Aesar, NBS 127, UA Acros, and UTSA Acros. NIST 120c was also analyzed as a quality control standard. The stable oxygen isotope results are reported in ratios of heavy to light and expressed relative to a standard in the per mil unit (‰). V-SMOW (Vienna Standard Mean Ocean Water) is the standard for stable oxygen isotope reporting. Delta notation

is used for discussing the results, where a positive $\boldsymbol{\delta}$ value means that the ratio of heavy to light isotopes is higher in the sample than it is in the standard, also known as "enriched", while a negative $\boldsymbol{\delta}$ value means that the ratio of heavy to light isotopes is lower in the sample than it is in the standard, also known as "depleted" (e.g., McKinney et al., 1950; Sharp, 2017).

The oxygen isotope trends were compiled by manually splicing individual tooth records to build a longer-term record using a combination of the morphological staggered replacement pattern in Caldwell (2006) and the isotopic record (see Appendix C). The record represents approximately 7 months. This is calculated from the growth time of each tooth, which is based on the duration of individual growth bands from previous studies (Gren and Lindgren, 2013), and accounting for the offset of each tooth record when correlated and spliced. The hypothesis that the isotopic dataset found in Alabama mosasaur teeth will show trends in mosasaur paleoecology by reflecting their occupation of distinct water sources was tested through analysis of patterns in the tooth records and comparison to previous analysis of *Platecarpus* mosasaurs.

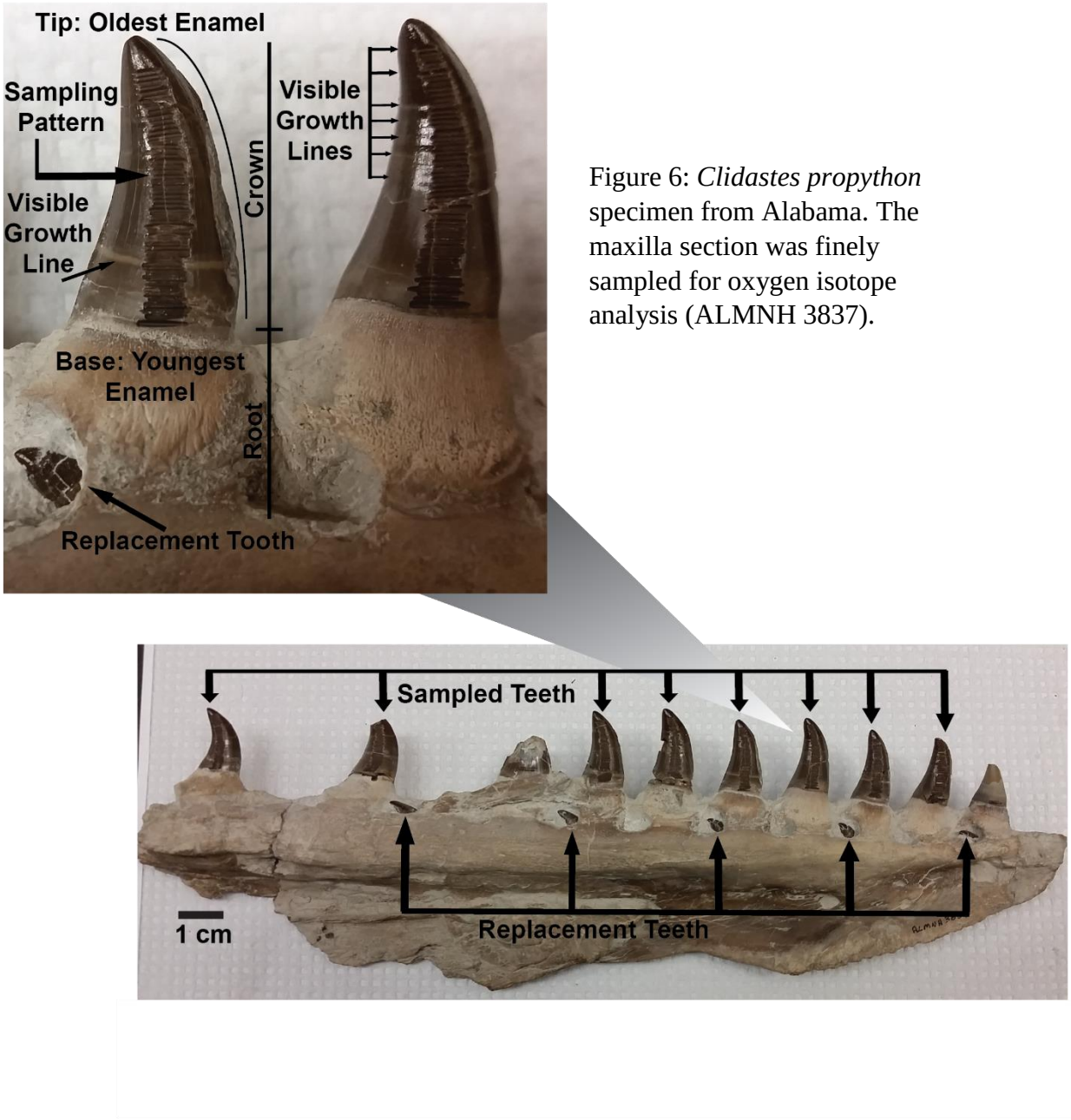

Figure 6: *Clidastes propython* specimen from Alabama. The maxilla section was finely sampled for oxygen isotope analysis (ALMNH 3837).

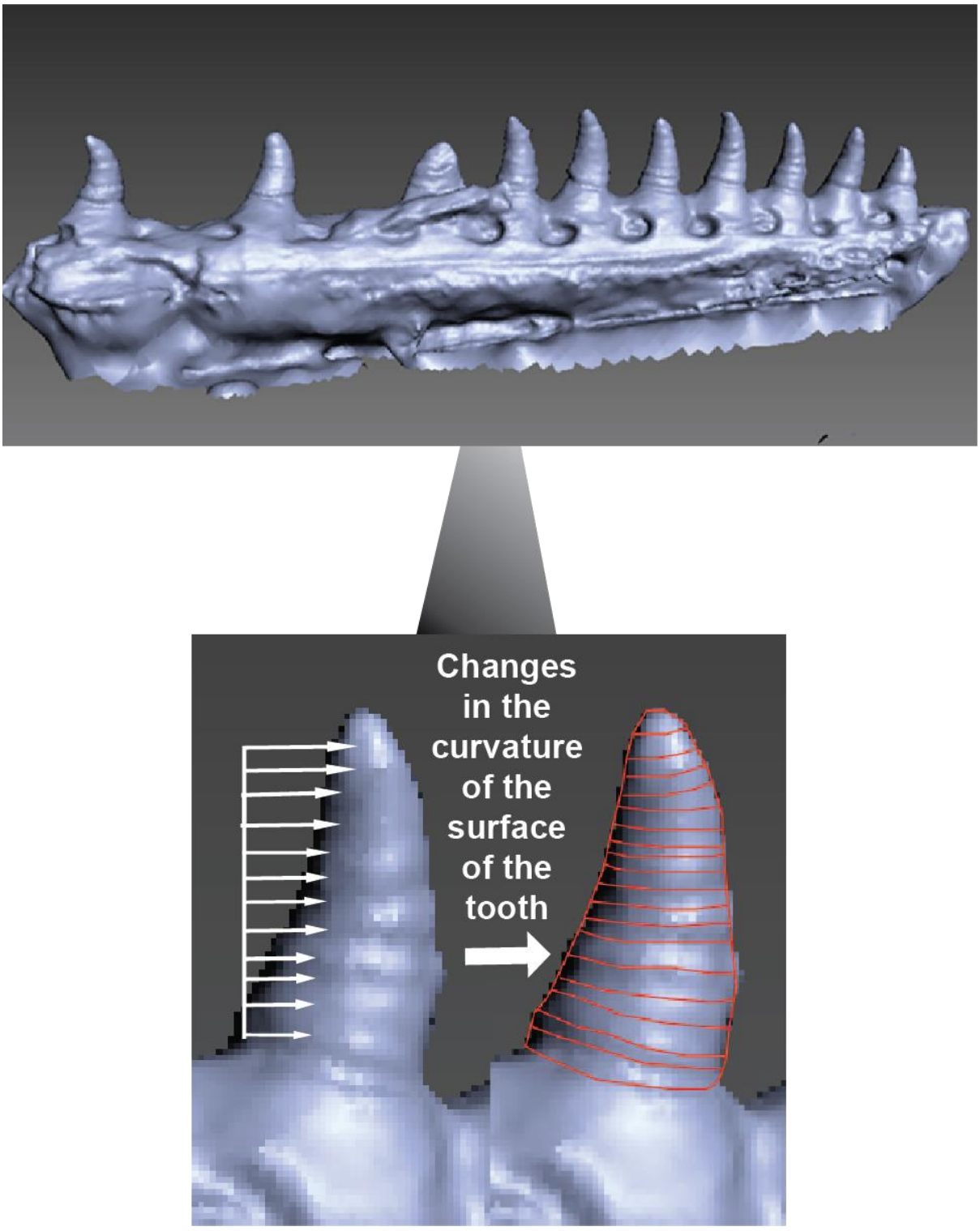

Figure 7: Pre-sample 3D scan of *Clidastes propython* specimen showing changes in the curvature of the teeth that serves as an indicator of growth increments.

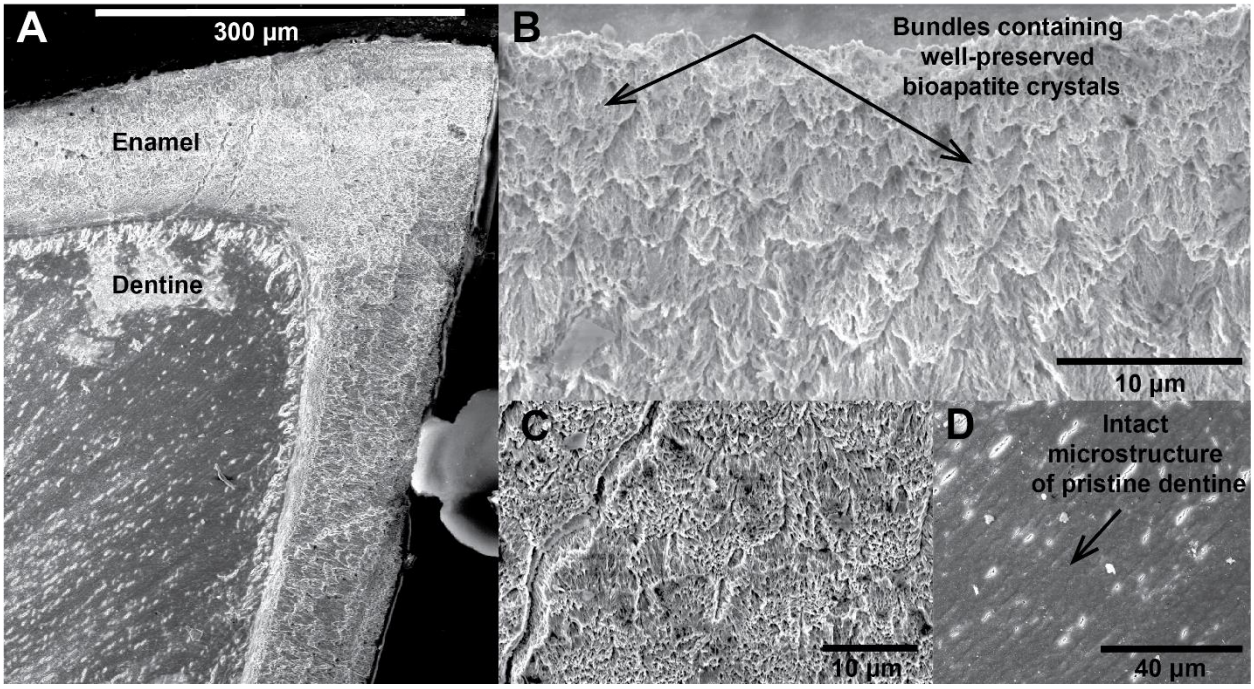

Figure 8: Scanning electron micrographs (SEM) of *Clidastes propython* associated fossil tooth enamel (A-C). Note bundles containing bioapatite crystals, indicating exceptional preservation. Additionally, in this specimen even the dentine is pristine, with characteristic wave-like microstructure intact (D).

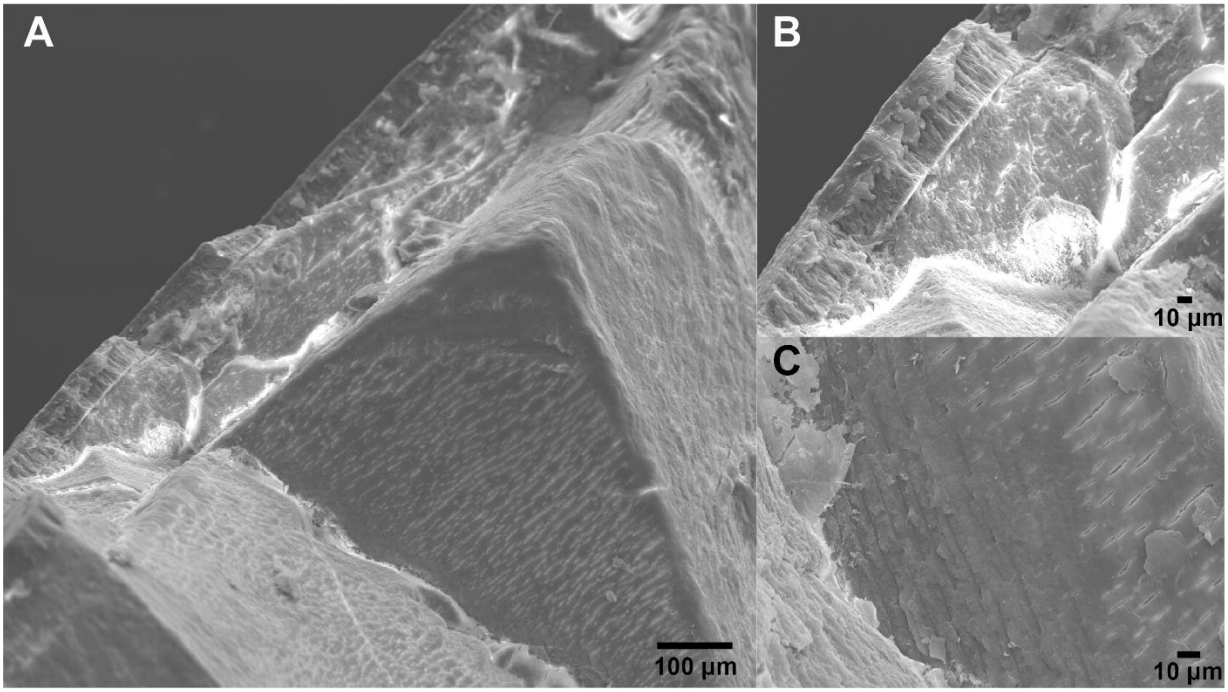

Figure 9: Scanning electron micrographs (SEM) of *Clidastes propython* sampled fossil tooth enamel (A-C). The sampled enamel also contains the characteristic microstructure indicating exceptional preservation and shows no signs of alteration.

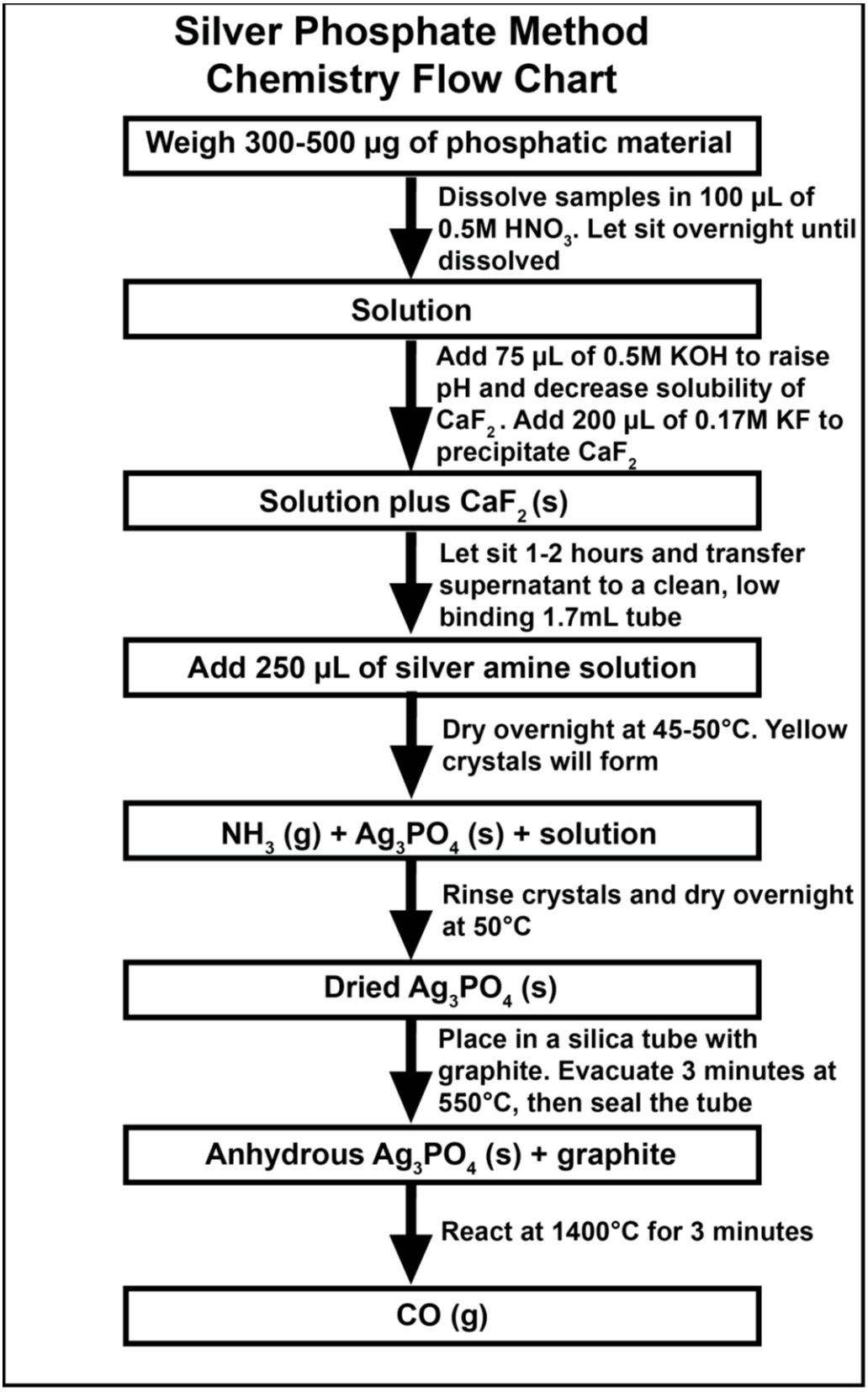

Figure 10: Silver Phosphate Method flow chart. Image modified after O'Neil et al., 1994.

RESULTS

Isotopic Results

Results of each individual tooth from the *C. propython* maxilla are summarized in Figure 11 and in Appendix A. Tooth #3 has three negative spikes in $\delta^{18}O$, one at the base of the tooth, the second near the middle, and the third near the crown tip. All three depletions are between 1.5‰ and 2.0‰ in amplitude. In addition to the superimposed excursions, $\delta^{18}O$ remains relatively constant throughout the tooth at ~22.5‰ until decreasing to ~21.0‰ near the base. Tooth #4 contains an overall increase in $\delta^{18}O$ from ~20.5‰ near the crown tip to ~22.0‰ at the base of the tooth. Superimposed on this is one negative spike of ~1.5‰ amplitude near the base. Two other minor negative spikes are observed near the tip, one of ~1.0‰ amplitude and the other less than ~1.0‰ amplitude. Tooth #5 has an overall increase in $\delta^{18}O$ from 20.5‰ at the crown tip to ~21.5‰ near the base of the tooth. Superimposed are two prominent negatives spikes, the first of which occurs approximately 2/3 of the way down from the crown tip of the tooth and the second of which occurs approximately in the middle of the tooth, with amplitudes of ~1.5‰ and ~2.0‰, respectively (Fig. 12). Tooth #6 contains an overall increase in $\delta^{18}O$ from ~19.0‰ near the crown tip of the tooth to ~21.5‰ near the middle, then an overall decrease to ~20.5‰ near the base. Superimposed are two negative spikes and one positive spike. The positive spike is ~1.5‰ in amplitude and occurs in the middle of the tooth. The first negative spike of ~1.5‰ amplitude occurs near the base of the tooth. The second negative spike is ~4.0‰ in amplitude, which is the largest in all the teeth, and it occurs near the base of the tooth. Tooth #7 has a stepwise decrease in $\delta^{18}O$ from ~22.0‰ near the crown tip to ~21.5‰ near the base, with a superimposed positive

spike of ~1.5‰ amplitude just below the crown tip and a positive spike of ~1.0‰ amplitude above the base of the tooth. Tooth #8 has a large negative spike of ~3.5‰ amplitude at the base of the tooth, a positive spike of ~2.0‰ amplitude approximately 2/3 of the way up from the base, and another negative spike of ~1.0‰ amplitude just below the crown tip. In addition, there is a gradual overall increase from the crown tip to the base in $\delta^{18}O$ from ~20.5‰ to ~21.5‰. Tooth #11 contains an overall decrease in $\delta^{18}O$ from ~20.5‰ near the crown tip of the tooth to ~19.5‰ near the middle, then an overall increase to ~21.5‰ near the base of the tooth. Superimposed on the overall trend is a negative spike of ~2.5‰ amplitude near the base of the tooth and two positive spikes of ~1.0‰ amplitude near the middle. Lastly, Tooth #13 has an overall constant $\delta^{18}O$ average of ~19.5-20.0‰, with a negative spike of ~1.0‰ amplitude near the crown tip, a positive spike of ~1.0‰ amplitude approximately 1/3 of the way down from the crown tip, and two other positive spikes of ~1.0‰ amplitude near the middle of the tooth.

Tooth Correlation and $\delta^{18}O$ Trends

All of the teeth are plotted together to observe overall trends in Figure 13. The teeth are then offset with respect to positions in the jaw following tooth replacement patterns (see Appendix C; Bertin et al., 2018; Delgado et al., 2013) and correlating $\delta^{18}O$ trends. The correlated tooth records represent a combined and spliced long-term record of $\delta^{18}O$ for the *C. propython* individual (Appendix C; Fig. 14). It is important to note that the negative excursions align independent of the isotopes being spliced; this exceptional correlation is achieved by using the anatomical model of splicing described in Appendix C, rather than using the excursions alone to correlate the record. There are two primary trends observed in the spliced record: 1.) superimposed on an overall trend are semi-regular negative excursions in $\delta^{18}O$ that occur approximately every 12-20 days, are well correlated in all spliced teeth, and are up to ~4.0‰ in amplitude, and 2.) $\delta^{18}O$ gradually decreases

from ~21.5‰ to ~20.0‰, and remains relatively constant until 1/3 of the way through the record, then gradually increases to ~22.0‰ before a final sharp decrease to ~20.0‰.

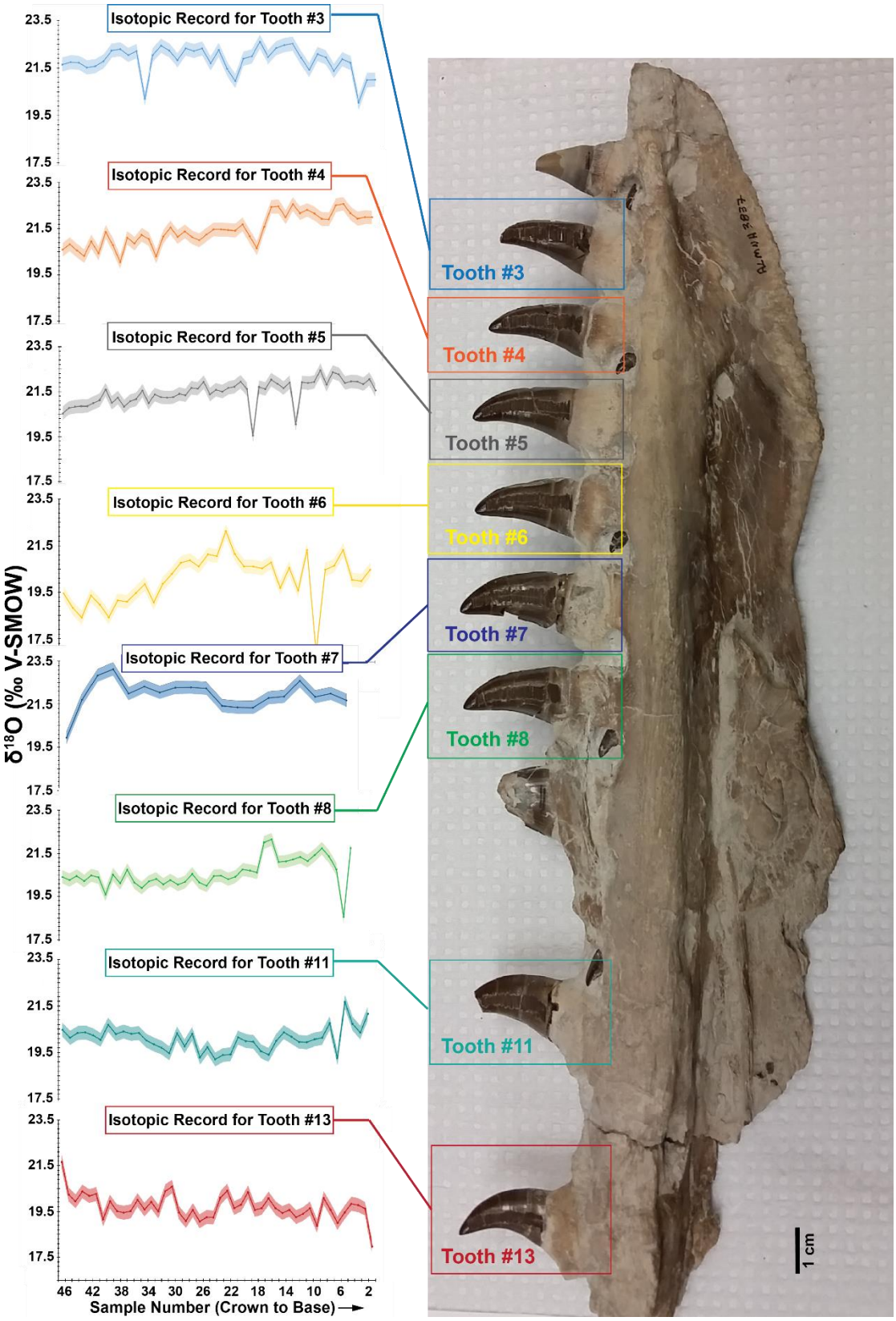

Figure 11: Isotopic analysis results for each tooth.

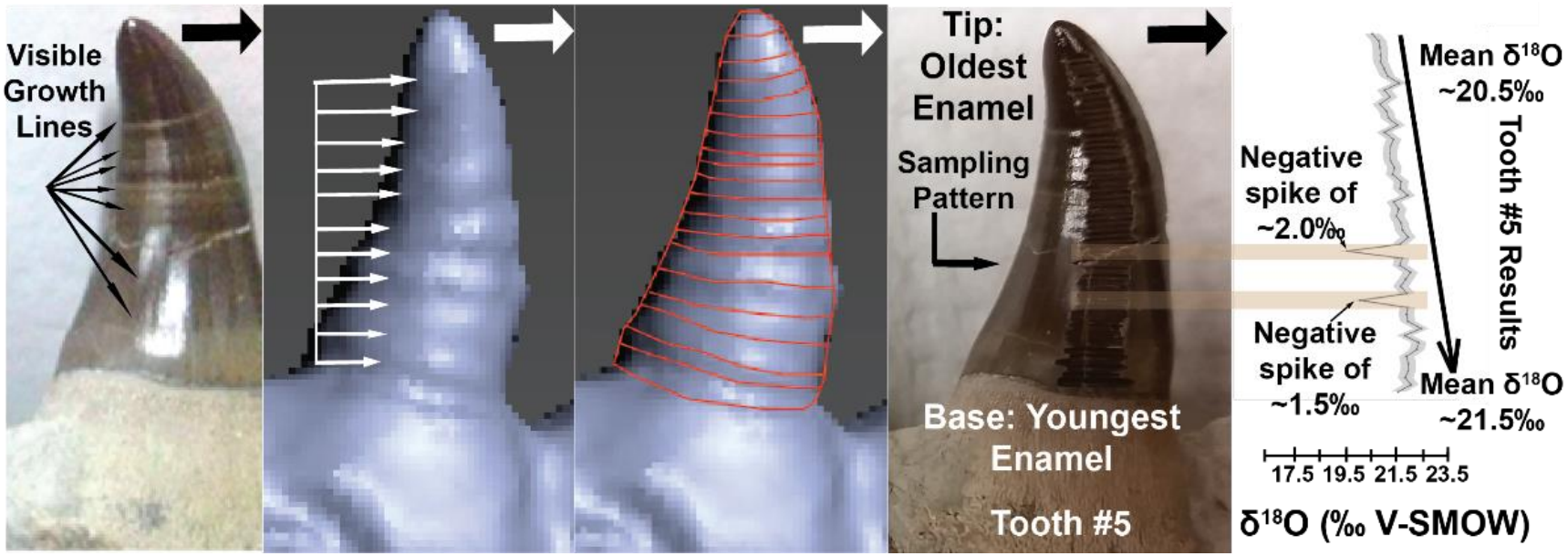

Figure 12: Visible external growth lines of the *C. propython* Tooth #5, from a white light photo (a) and 3D scan before sampling (b, c) and after (d). Oxygen isotope results are plotted alongside the tooth (e), with negative excursions highlighted. This process was performed for each tooth and plotted together vs. growth line increments (see Appendix A).

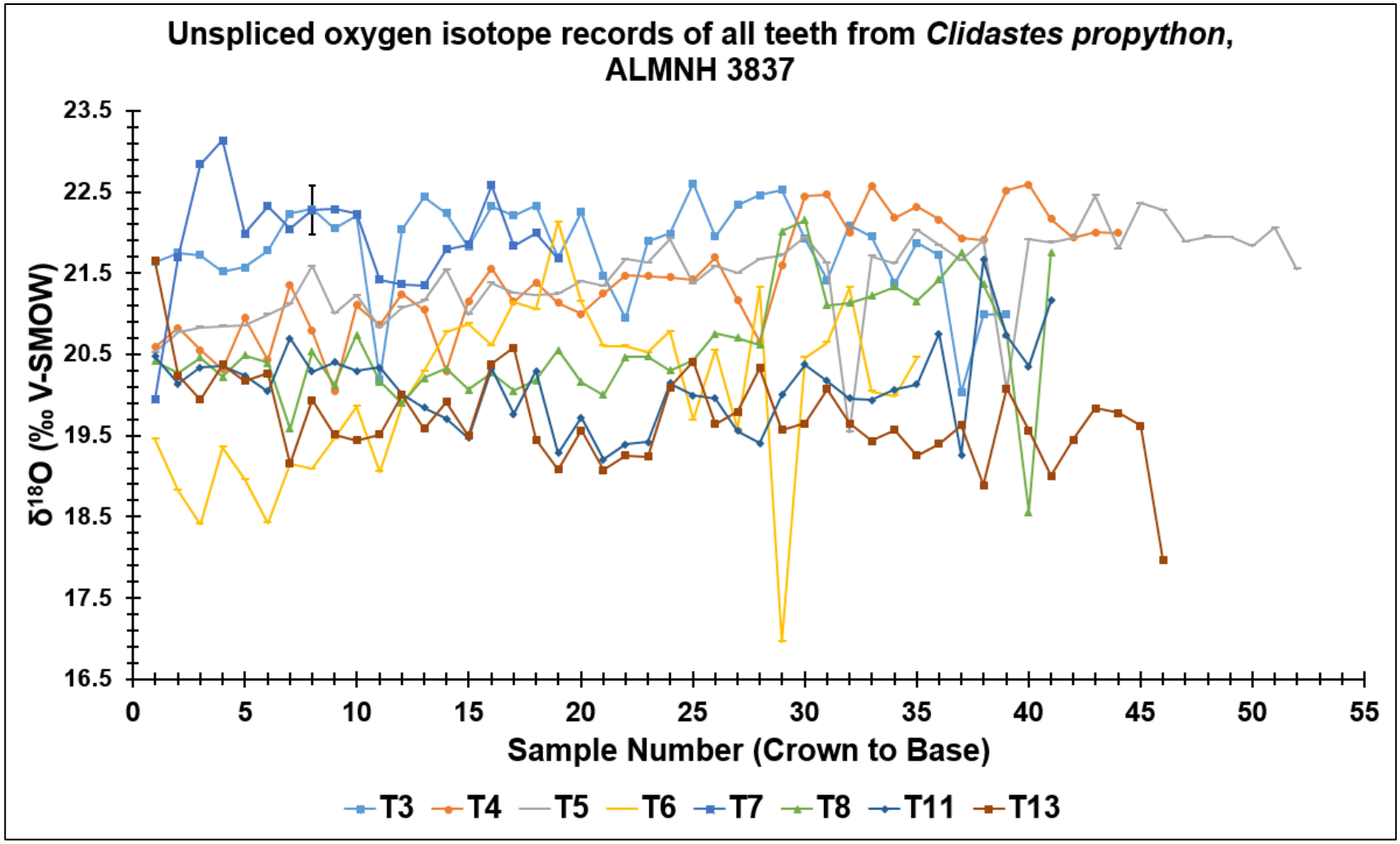

Figure 13: Isotopic analysis results, plotted without correlation. Analytical precision is represented on data point #8 of tooth #7.

DISCUSSION

Clidastes Paleoecology

The isotopic records from all eight consecutive teeth in the Alabama *Clidastes* mosasaur correlate well and were spliced to build a longer record. The two main trends seen in the $\delta^{18}O$ record show changes in the isotopic composition of the water the mosasaur inhabited (Fig. 14). In regards to the first trend, the superimposed negative excursions in $\delta^{18}O$ are pronounced and short-term, and occur approximately every 12 to 20 days (~2 weeks). This is contrary to a gradual increase or decrease in $\delta^{18}O$ that would be expected if they were the result of long-range mosasaur migration. Therefore, these short negative excursions of up to 4.0‰ in amplitude can be distinguished from paleomigration, and suggest four potential causes: 1.) diving into deeper, more ^{18}O depleted water during their inhabitation of open ocean environments, 2.) sampling or analysis artifacts, 3.) mosasaurs thermoregulation – if they were only partially endothermic or ectothermic, then internal temperature fluctuations may be driving the excursions, and 4.) incursion into water bodies with depleted freshwater sources, namely estuaries or rivers. Mosasaurs are known to possess a light-sensing organ on their heads called a parietal eye (Connolly, 2016), which would aid in diving, and the vertebrae of some genera of mosasaurs were found to show the presence of avascular necrosis, a direct indicator of decompression syndrome from diving (Rothschild and Martin, 1987). *Clidastes spp.* do not show the presence of avascular necrosis, however, and they have one of the smallest parietal eyes of the mosasaur genera (Connolly, 2016; Rothschild and Martin, 1987), suggesting that deep diving was an unlikely characteristic behavior of the *Clidastes spp*. (Massare, 1994). Additionally, the parietal

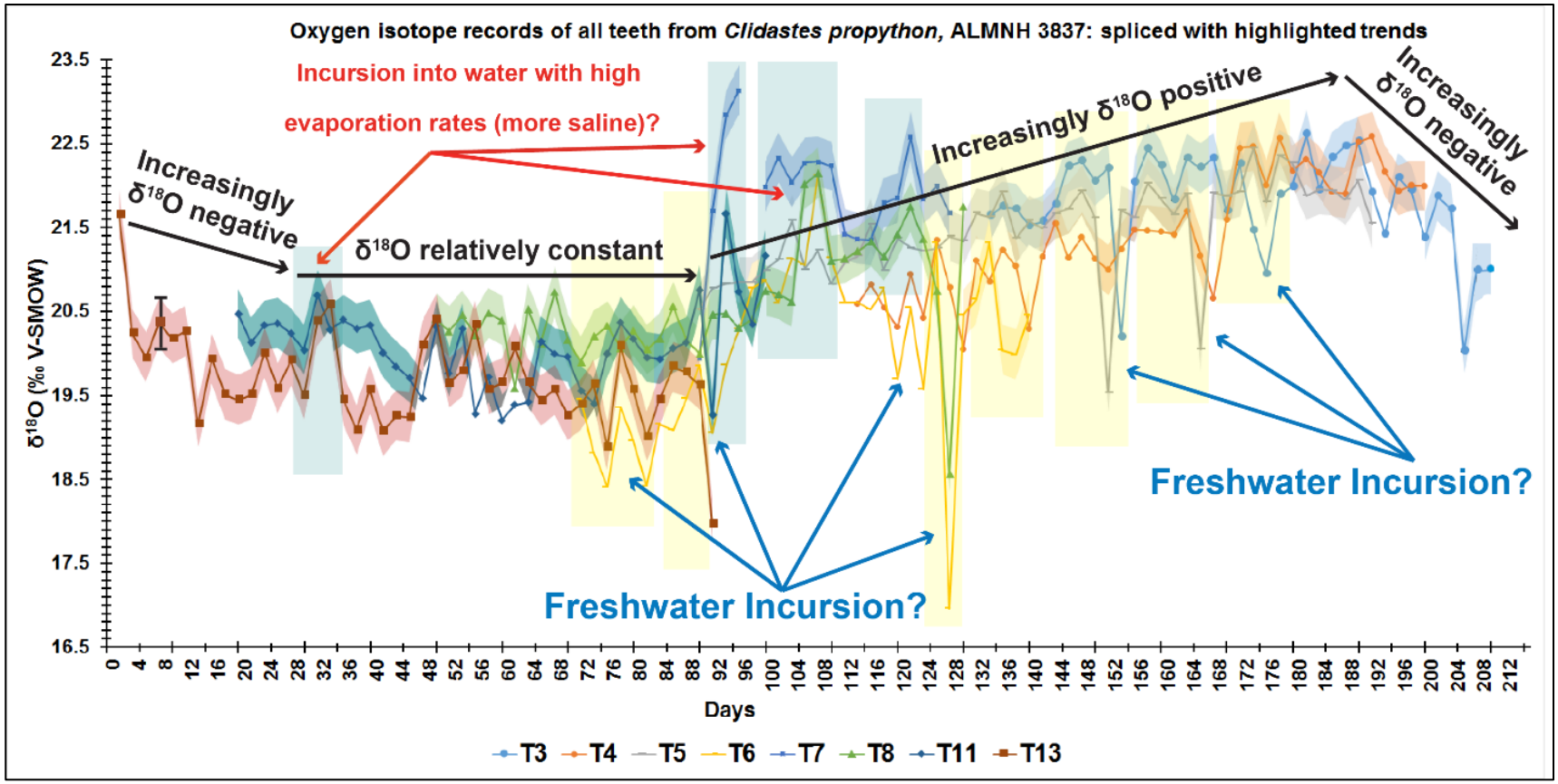

Figure 14: Isotopic analysis results, plotted together – spliced with highlighted trends. Yellow shaded boxes represent negative excursions of at least 1.0‰; blue shaded boxes represent positive excursions of at least 1.0‰. T3, T4, T5, T6, T7, T8, T11 and T13 refer to Tooth #3, #4, #5, #6, #7, #8, #11, and #13, respectively. Analytical precision is represented on data point #4 of tooth #13 and with the shaded error bands.

eye may also function for navigation and orientation related to migration (Connolly, 2016), so the presence of one does not necessarily indicate diving habits. Furthermore, metabolism generally slows when animals dive, regardless of their thermoregulation, as has been shown in seals and whales (Kooyman and Castellini, 1980), as well as leatherback turtles (Standora et al., 1984). Therefore, even if the *Clidastes propython* individual dove frequently to great depths, it is unlikely that the organism precipitated enamel during the dive due to plummeting metabolic rate. Modern diving animals rarely dive for more than an hour at a time; for example, only 5% of analyzed whale dives lasted more than 30 minutes (Kooyman and Castellini, 1980) and observed seal dives average 204 seconds, with varying durations between 240 and 2,220 seconds (3-37 minutes; Blanchet et al., 2015; Hückstädt et al., 2018). Thus, even if the organism was precipitating enamel during diving, the amount of time spent in the deep, depleted ocean bottom would likely be inadequate to precipitate enough enamel to significantly influence the isotopic composition of the precipitated tooth enamel. In regards to the second potential cause, sampling or analysis artifacts, the samples that contained negative excursions were examined thoroughly. The samples were systematically collected and treated, and the low $\delta^{18}O$ samples were checked for any evidence of potential sampling artifact sources, such as drilling depth, possible contamination, and imperfections on the sampled enamel surface. No analysis artifacts were found, and thorough standard calibration gives high confidence in the data set. Importantly, the negative excursions align independently of the isotopes being spliced. Correlation solely through use of the anatomical model of splicing (described in Appendix C) lends high confidence that these negative spikes are real and not the result of sampling or analytical artifacts. Furthermore, many of the negative spikes have samples preceding or proceeding them that contain decreases or increases in $\delta^{18}O$ leading to or from the excursion, indicating that the primary excursion

sample is reporting a reliable $\delta^{18}O$ value. Lastly, as will be discussed in much more detail, the Kanses *P. ictericus* study by Totten (2009) showed similar negative excursions in $\delta^{18}O$, suggesting these negative spikes to be a result of a paleoecological signal, not artifacts.

To address the question of mosasaur thermoregulation influencing the record, body temperature calculations were performed to investigate whether internal temperature fluctuations may be driving the excursions if they were only partially endothermic or ectothermic (Appendix B; Lécuyer et al., 2013). Averaging the values of the negative excursions (~3.0‰), body temperature was calculated for the mosasaur body during an excursion and for the average not during an excursion. A calculated 13.2°C temperature change is necessary to create the average $\delta^{18}O$ value of the excursions if it were fractionation due to daily temperature fluctuation. Modern aquatic ectothermic reptiles, for example snapping turtles, have been found to have daily temperatures that differ in most cases by 1 to 2°C, and thus have a relatively stable body temperature throughout the day, even when moving through waters of different temperatures (Fitzgerald and Nelson, 2011). It is unlikely that mosasaurs would have experienced ~13°C daily temperature fluctuation, particularly in the warm Late Cretaceous ocean. Furthermore, the negative excursions occur approximately every two weeks, not daily, so daily temperature fluctuations do not appear to be the source of the negative excursions.

The cause for the bi-weekly pattern of negative excursions in $\delta^{18}O$, therefore, is likely incursion into freshwater sources including coastal estuaries and rivers. The regularly spaced negative $\delta^{18}O$ excursions are strikingly similar to the foundational study for this research on Kansas *Platecarpus ictericus* specimens, which also interpreted the negative $\delta^{18}O$ spikes in the record as freshwater incursions by the mosasaurs (Totten, 2009). Due to Rayleigh fractionation, meteoric water, and thus freshwater, has a much lower $\delta^{18}O$ composition than marine

environments and will stand out in the isotopic record from material dominantly precipitated in a marine setting. Several rivers drained into the ME and central WIS, and these rivers and their associated coastal estuaries would have been readily accessible to the mosasaurs, who were agile swimmers. Therefore, it is most likely that the short-term negative $\delta^{18}O$ excursions of 1.0 to 4.0‰ amplitude in the isotopic record is the *C. propython* individual traveling approximately every 12 to 20 days to freshwater habitats in the ME.

If this is the case, why then did both the Kansas *P. ictericus* (Totten, 2009) and the Alabama *C. propython* (this study) travel to freshwater sources periodically? Modern sea snakes, living relatives of the mosasaur, drink freshwater periodically to stay hydrated (Lillywhite et al., 2008). The 12 to 20 day regularity of freshwater incursions in two different mosasaur genera and in two distinct regions of the Late Cretaceous seaway indicates that a biological need, such as drinking freshwater to osmoregulate, motivated the mosasaurs' frequent trips to coastal and river environments. Modern pelagic sea snakes can go up to six months without drinking freshwater while waiting for rainfall to occur during the dry season; however, neritic sea snakes near available sources of freshwater may drink much more frequently (Lillywhite et al., 2008). Mosasaurs, being agile swimmers with many nearby sources of freshwater, may have drank water more often than their sea snake relatives. Additionally, they may also have frequented the freshwater systems to feed (Russell, 1967), taking advantage of the plentiful prey and restricted space that a river system would have to offer. How often they would have fed is unknown, but if they were endothermic as suggested by Harrell et al. (2016), they would have likely fed more frequently than their modern ectothermic land-inhabiting relatives, komodo dragons. Like modern lizards, however, it is suggested that mosasaurs may have been territorial (Everhart, 2008; Lingham-Soliar, 2004). While territorial behavior is less common for pelagic predators, if

mosasaurs were migrating into restricted river system environments it may have influenced their behavior and made full time residence in such restricted spaces untenable.

Well-correlated and irregular positive $\delta^{18}O$ peaks are also present in the record (Fig. 14). The positive $\delta^{18}O$ excursions likely resulted from mosasaur incursion into nearby restricted, more saline environments, namely lagoons, which are enriched due to evaporative effects on $\delta^{18}O$ fractionation. Seeking salt water lagoons is another strategy for osmoregulation; if there is not a nearby source of freshwater, it is suggested that modern sea snakes can drink from the up to 20 m thick freshwater lens that forms on the surface of lagoons or the ocean after a heavy rainfall event, which can last for several days in calm lagoons (Lillywhite et al., 2008). It is possible that mosasaurs, the relative of sea snakes, had similar behaviors. In the *C. propython* $\delta^{18}O$ record, the two most prominent and well-correlated positive $\delta^{18}O$ spikes are followed by negative $\delta^{18}O$ spikes. It is plausible that the mosasaur inhabited an enriched, saline lagoon (positive spike in $\delta^{18}O$) while waiting for a rainfall event, then drank the depleted freshwater lens for potentially days afterwards (subsequent negative spike in $\delta^{18}O$).

Lastly, mosasaurs may have migrated into restricted waters (either freshwater systems or lagoons) for breeding purposes. Fully marine organisms of the modern ocean, such as sea turtles and dolphins, migrate to shallow, protected areas to breed and give birth (Hays and Scott, 2013; Weir, 2008). Fossil occurrences in shallow estuarine and fluvial depositional environments on several continents generally support some mosasaur inhabitation of these environments (Lindgren and Siverson, 2004; Russell, 1967). It is unlikely, however, that during breeding and pregnancy mosasaurs were precipitating enamel due to bodily resources going towards sustaining offspring; for example, biomineralization is impacted in marine mammals by the physiological requirements of pregnancy (Newsome et al., 2010). Regardless, the 12 to 20 day

recurrence interval is much too frequent to be explained by breeding-related migration alone.

In regards to the secular trend seen in the *C. propython* $\delta^{18}O$ record, there are a few possible interpretations. Mosasaurs potentially have migratory behavior (Totten, 2009; Lindgren and Siverson, 2004), which may explain the multi-month $\delta^{18}O$ record. The gradual shifts in $\delta^{18}O$ indicates progressive migration into ^{18}O enriched water, such as migration into cooler water, or migration into evaporitic environments. The mosasaur may have inhabited warmer waters at the beginning of the record, accounting for the overall lower $\delta^{18}O$, and migrated into colder waters, reflected by higher $\delta^{18}O$, before finally migrating back to warmer waters of lower $\delta^{18}O$ near the end of the record (Fig. 14). Temperature variations within the central WIS and the ME are predicted to have been ~3°C, based on turtle and fish bone calculations (Coulson et al., 2011), as well as Late Cretaceous temperature gradients (Amiot et al., 2004). The difference in $\delta^{18}O$ from the beginning to the middle of the *C. propython* record is ~3.0‰, which would require a ~13.9°C temperature change based on temperature calculations for biogenic apatite (See Appendix B; following Pucéat et al., 2010). Therefore, the temperature change required for this trend could not have been obtained by migrating within the seaway, as was suggested for Kansas *P. ictericus* individuals (Totten, 2009). Furthermore, over the interval of long-term increase in the *C. propython* $\delta^{18}O$, the superimposed negative excursions in $\delta^{18}O$ become less negative, decreasing from excursions of ~4.0‰ amplitude at the start to ~2.0-2.5‰ amplitude (Fig. 14). If the mosasaur were migrating into colder water, the freshwater incursion-produced negative spikes should become more prominent, because, as the mosasaur moved slowly into colder water, the difference in $\delta^{18}O$ between the freshwater and the marine water should become more pronounced, in particular because higher latitudes in the WIS were predicted to have freshwater sourced from isotopically light runoff originating from the mountain range on the western side of

the seaway (Dettman and Lohman, 2000). This is not the case, however, so we must look to other potential interpretations.

I also considered that the long-term, multi-month *C. propython* $\delta^{18}O$ trend may reflect changing $\delta^{18}O$ with seasons. The Late Cretaceous was characterized by low seasonality, however, with estimated maximum temperatures as high as 35 to 37 °C and relatively low seasonal variability of 7 to 12 °C (Steuber et al., 2005). As stated above, the $\delta^{18}O$ shift in the *C. propython* bioapatite would require a ~13.9°C temperature change, which seems unlikely if the seasonal variability is 7 to 12 °C. Seasonality within the specific time interval is not well constrained, however, and cannot be ruled out based on existing models, especially in regard to the 7-month time frame of mosasaur tooth accretion.

As discussed previously, $\delta^{18}O$ water composition is a marker of salinity and therefore will be recorded in the mosasaur record. The long term increase in the *C. propython* $\delta^{18}O$ most likely records progressive migration into environments that are more evaporitic and more enriched in ^{18}O. The interpretation I favor, therefore, is that the mosasaur inhabited open marine water at the beginning of the record, accounting for the overall lower $\delta^{18}O$ value, then the mosasaur migrated into more restricted, saline, evaporitic waters with a higher $\delta^{18}O$ value. The ME was a restricted environment due to its paleogeography (Coulson et al., 2011), so the mosasaur probably migrated to the more proximal and shallow setting of the ME from the more distal, open ocean WIS and/or ancestral GOM. This interpretation corroborates the superimposed negative $\delta^{18}O$ excursions becoming increasingly less negative over the multi-month record. The open central WIS, where the freshwater would have likely been sourced from precipitation on the high-altitude mountains on the western side of the seaway (Dettman and Lohman, 2000), would have freshwater with a lower $\delta^{18}O$ value than freshwater from the ME area, which was

likely sourced from low-altitude continental runoff. Therefore, as the mosasaur migrated further into the ME, this difference would have caused the negative $\delta^{18}O$ excursions (interpreted as freshwater incursions) to become increasingly less negative as the mosasaur migrated from the less evaporative, open WIS. Accounting for both the long-term trend and the short-lived excursions, this is the model that best fits the *C. propython* $\delta^{18}O$ data, suggesting that the mosasaur individual migrated into the restricted ME from the open WIS, and periodically drank freshwater along its path.

These data support prior work suggesting that mosasaurs were migratory animals. As mentioned above, the foundational study for this thesis suggested that *Platecarpus ictericus* mosasaurs from Kansas exhibited migratory behavior and freshwater incursion from phosphate $\delta^{18}O$ records in tooth enamel (Totten, 2009). Recent isotopic evidence for thermoregulation of three different mosasaur genera suggest that mosasaurs had a wide habitat range, with body temperature regulation facilitating migration into a wide variety of waters, such as high-latitude polar waters; furthermore, this study considered gigantothermy, but concluded it was not the controlling factor on the elevated body temperatures, with there being no relationship between mosasaur body size and calculated temperature (Harrell et al., 2016). Additionally, mosasaur fossils have been found on every continent, including Antarctica (Russell 1967; Martin et al., 2002; Harrell and Pérez-Huerta, 2015; Ross, 2009), while ectothermic reptiles in polar regions are rare even in a greenhouse world (de la Fueta et al., 2010); therefore, the adaption of endothermy likely enabled mosasaurs to conquer every continent, and even migrate between them. *Clidastes* mosasaurs from Sweden are interpreted to have originated from the ME (Lindgren and Siverson, 2004), suggesting they had long migratory range, similar to sharks and whales today; for example, modern sharks have been observed to travel up to 2800 km in a little

over a month (Kohler et al., 2002), while seasonal migration of whales triggers continuous movement, which can amount to over 2000 km after only one month into their voyage (Horton et al., 2011).

Clidastes vs. *Platecarpus* Paleoecology

There are two primary differences in the isotopic record of the Alabama *Clidastes propython* versus the Kansas *Platecarpus ictericus* mosasaurs (Fig. 15). The mean $\delta^{18}O$ value differs between the Kansas *P. ictericus* and the Alabama *C. propython*, with 17.1‰ (S.D. = 0.6‰, n = 86) for the *Platecarpus* and ~20.8‰ (S.D. = 1.0‰, n = 317) for the *Clidastes*. I interpret the ~3.7‰ difference in oxygen isotope composition to reflect niche partitioning related to the more evaporative, lower latitude habitats of the ME versus the open, central WIS. In addition, Totten demonstrated that the *Platecarpus ictericus* migrated southward up to several hundred kilometers (2009). My results indicate that the Alabama *Clidastes propython* also migrated; however, the individual migrated within the environments of the ME and surrounding Southern Interior Subprovince of the WIS and may have been shorter range than the Kansas *Platecarpus* mosasaurs, at least during the period of tooth accretion that is preserved at the end of the study specimen's life. Distinct differences in migratory behavior could be a potential consequence of the size disparity between the *Clidastes* and the *Platecarpus* (Russell, 1967). The key similarity between the isotopic record of the *C. propython* and the *P. ictericus* is that both exhibit semi-regular, well-correlated negative excursions of 1.0 to 4.0‰ in amplitude. The periodicity of the negative $\delta^{18}O$ excursions in the adult *P. ictericus* mosasaur record and the *C. propython* record further implicates the possibility that osmoregulation, which would undoubtedly be a shared trait at the family level, required adult mosasaurs to ingest freshwater on a regular basis.

Implications for Anatomical Models of Mosasaur Tooth Replacement Patterns

Amniotes, which include reptiles, do not replace their teeth randomly; it is accomplished through organized patterns (Edmund, 1969; Wong, 2011; Bertin et al., 2018). Correlation of the isotopic data was attempted using the two main modes of amniote replacement patterns: 1.) the sequential pattern, which is when the teeth are replaced consecutively throughout the jaw in a wave, where either the anterior replacement teeth are further along than the posterior teeth, or vice versa, and 2.) the alternate pattern, where two waves of dental replacement, one for even positions and the next for odd positions, proceed across the jaw (Bertin et al., 2018). The alternate pattern has typically been described for modern reptiles (Edmund, 1969; Wang et al., 2006; Bertin et al., 2018); however, the isotopic data obtained from the teeth in the *Clidastes* jaw correlate well when the contiguous sequential mode of tooth replacement is used to align the records, which is in contrast to the typically suggested alternate mode of tooth replacement for reptiles (Appendix C; Bertin et al., 2018). Additionally, the type of sequential pattern that results in a successful correlation is the replacement of the posterior teeth first, followed by the anterior teeth in a gradient. These unbiased isotopic data demonstrate that the *Clidastes* mosasaur individual may have replaced their teeth using the sequential pattern rather than the alternate pattern. If so, this may imply that the sequential mode of tooth replacement evolved in certain reptilian lines, rather than mammals exclusively. Otherwise, a more complex form of the alternate pattern may have been in place, such as the spacing of the alternate and even replacement waves allowing for the pattern to become nearly sequential. More studies investigating mosasaur tooth replacement waves, and incorporating geochemical tools to do so, should be performed to confirm if this is observed anatomically across mosasaur genera.

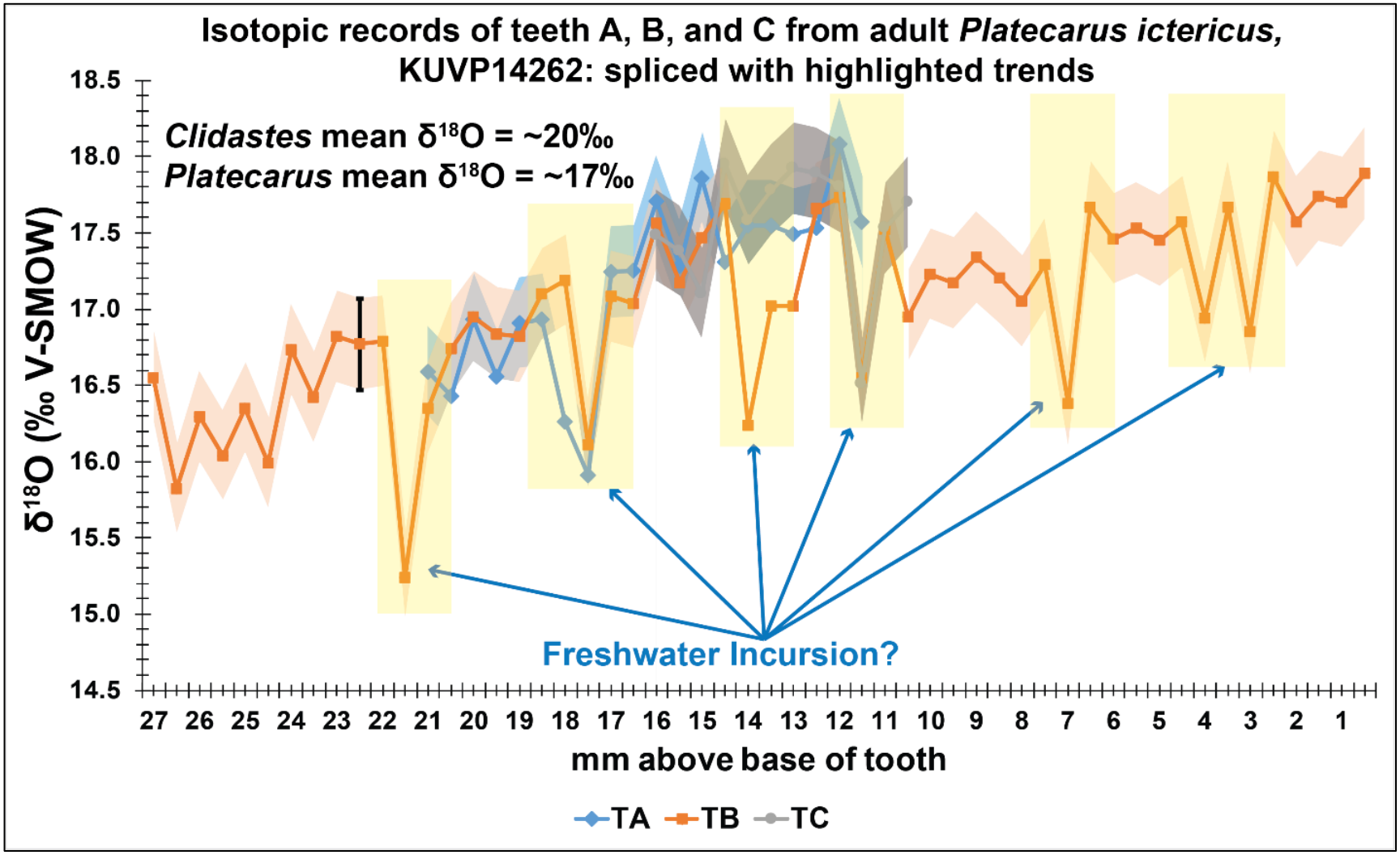

Figure 15: Kansas *Platecarpus ictericus* isotopic analysis results, plotted together – spliced with highlighted trends. Yellow shaded boxes represent negative excursions of at least 1.0‰. TA, TB and TC refer to Tooth A, B and C, respectively. Analytical precision is represented on data point #10 of tooth B and with the shaded error bands (modified from Totten, 2009).

CONCLUSIONS

Here I present evidence that the extinct marine reptiles called mosasaurs from the Late Cretaceous of North America likely migrated within both the Mississippi Embayment and the Western Interior Seaway. Oxygen isotope records from eight consecutive teeth within an adult *Clidastes propython* right maxilla from the Mooreville Chalk, Alabama correlate well and were spliced to build a multi-month record of water composition in which the individual was living. I am confident that the original fossil material is well preserved, due to the consistent trends across teeth and the exceptional preservation of bioapatite microstructures imaged with SEM. The $\delta^{18}O$ record verifies other evidence that indicates mosasaurs may have been migrators, namely fossil evidence (Lindgren and Siverson, 2004), and isotopic evidence (Harrell et al., 2016; Totten, 2009). The disparate $\delta^{18}O$ records of the Alabama *Clidastes* mosasaur versus the Kansas *Platecarpus* support the hypothesis that their distributions are related to the differing habitats of the Mississippi Embayment and the central Western Interior Seaway. Similarities in regularly spaced negative $\delta^{18}O$ excursions in the Alabama *Clidastes propython* and the Kansas *Platecarpus ictericus* strongly suggest that mosasaurs were limited in osmoregulation and required periodic visits to freshwater sources for drinking and feeding like their living relatives, sea snakes. Understanding the paleobiology and paleoecology of mosasaurs, which lived in a greenhouse climate of the Late Cretaceous, may lend perspective not only on changing migration habits of large marine animals during climate warming and sea level rise acceleration, but also on the conservation of sea snakes, many species of which are currently endangered.

REFERENCES

Amiot, R., Lécuyer, C., Buffetaut, E., Fluteau, F., Legendre, S., and Martineau, F., 2004, Latitudinal temperature gradient during the Cretaceous Upper Campanian-Middle Maastrichtian: $\delta\ ^{18}O$ record of continental vertebrates: *Earth and Planetary Science Letters*, v. 226, p. 255-272.

Barrick, R.E., Showers, W.J., and Fischer, A.G., 1996, Comparison of Thermoregulation of Four Ornithischian Dinosaurs and a Varanid Lizard from the Cretaceous Two Medicine Formation: Evidence from Oxygen Isotopes: *Society for Sedimentary Geology*, v. 11, p. 295–305.

Bell, G. L., Jr., and Martin, J. E., 1995, Direct Evidence of Aggressive Intraspecific Competition in Mosasaurus conodon (Mosasauridae: Squamata), Journal of Vertebrate Paleontology, v.15(3), 18A.

Bertin, T.J., Thivichon-Prince, B., LeBlanc, A.R.H, Caldwell, M.W., 2018, Current Perspectives on Tooth Implantation, Attachment, and Replacement in Amniota: *Frontiers in Physiology*, v. 9, p. 1-20.

Blackburn, D.G., and Sidor, C.A., 2014, Evolution of viviparous reproduction in Paleozoic and Mesozoic reptiles: *International Journal of Developmental Biology*, v. 58, p. 935-948.

Blakey, R., 2017. Colorado Plateau Geosystems' new Website, DEEP TIME MAPS, Online available: https://www2.nau.edu/rcb7/

Blanchet, M.A., Lydersen, C., Ims, R.A., and Kovacs, K.M., 2015, Seasonal, Oceanographic and Atmospheric Drivers of Diving Behaviour in a Temperate Seal Species Living in the High Arctic: *PLoS ONE*, v. 10(7), p. 1-19.

Brusatte, S.L., Butler, R.J., Barrett, P.M., Carrano, M.T., Evans, D.C., Lloyd, G.T., Mannion, P.D., Norell, M.A., Peppe, D.J., Upchurch, P., and Williamson, T.E., 2014, The extinction of the dinosaurs: *Biological Reviews*, v. 2014, p. 1-15, doi: 10.1111/brv.12128.

Caldwell, M.W., 2006, Ontogeny, anatomy and attachment of the dentition in mosasaurs (Mosasauridae: Squamata): *Zoological Journal of the Linnean Society*, v.149, p.687-700.

Caldwell, M.W., and Lee, M.S.Y., 2001, Live birth in Cretaceous marine lizards (mosasauroids): *The Royal Society*, v. 268, p. 2397-2401.

Chinsamy, A., Tunoğlu, C., and Thomas D.B., 2012, Dental microstructure and geochemistry of *Mosasaurus hoffmanni* (Squamata: Mosasauridae) from the Late Cretaceous of Turkey: *Bull. Soc. géol. France,* v. 183, p. 85-92.

Clementz, M.T., and Koch, P.L., 2001, Differentiating aquatic mammal habitat and foraging ecology with stable isotopes in tooth enamel: *Oecologia*, v. 129, p. 461-472.

Clementz, M.T., Goswami, A., Gingerich, P.D., and Koch, P.L., 2006, Isotopic Records from Early Whales and Sea Cows: Contrasting Patterns of Ecological Transition: *Journal of Vertebrate Paleontology*, v. 26, p. 355-370.

Coulson, A.B., Kohn, M.J., and Barrick, R.E., 2011, Isotopic evaluation of ocean circulation in the Late Cretaceous North American seaway: *Nature Geoscience,* v. 4, p. 852–855.

de la Fuenta, M., Novas, F.E., Isasi, M.P., Lirio, J.M., Nuñez, H.J., 2010, First Cretaceous Turtle from Antarctica: *Journal of Vertebrate Paleontology*, v. 30(4), p. 1275-1278.

Delgado, S., Davit-Beal, T., Sire, J.Y., 2003, Dentition and Tooth Replacement Pattern in *Chalcides* (Squamata; Scincidae): *Journal of Morphology*, v. 256. p. 146-159.

Dettman, D.L. and Lohman, K.C., 2000, Oxygen isotope evidence for high-altitude snow in Laramide Rocky Mountains of North America during the Late Cretaceous and Paleogene: *Geology*, v.28, p. 243-246.

Dunson, W.A., and Ehlert, G.W., 1971, Effects of Temperature, Salinity, and Surface Water Flow on Distribution of the Sea Snake *Pelamis*: *Limnology and Oceanography*, v. 16, p. 845-853.

Edmund, A.G., 1969, Dentition, *in* Gans, C., Bellairs, A, and Parsons, T.S., eds., Biology of the Reptilia: Academic Press, London, v. I, p. 117–200.

Erickson, G.M., 1996, Incremental lines of von Ebner in dinosaurs and the assessment of tooth replacement rates using growth line counts: *Proc. Natl. Acad. Sci. USA*, v. 93, p. 14623-14627.

Everhart, M.J., 2001, Revisions to the Biostratigraphy of the Mosasauridae (Squamata) in the Smoky Hill Chalk Member of the Niobrara Chalk (Late Cretaceous) of Kansas: *Transactions of the Kansas Academy of Science*, v. 104(1-2), p. 59-78.

Everhart, M.J., 2008, A bitten skull of Tylosaurus kansasensis (Squamata: Mosasauridae) and a review of mosasaur-on-mosasaur pathology in the fossil record: *Transactions of the Kansas Academy of Science*, v. 111(3-4), p. 251-262.

Feduccia, A., 1973, Dinosaurs as Reptiles: *Society for the Study of Evolution*, v. 27, p. 166–169.

Field, D.J., Leblanc, A., Gau, A., and Behlke, A.D., 2015, Pelagic Neonatal Fossils Support Viviparity and Precocial Life History of Cretaceous Mosasaurs: *Palaeontology*, v. 58, p. 401–407.

Fitzgerald, L.A., and Nelson, R.E., 2011, Thermal biology and temperature-based habitat selection in a large aquatic ectotherm, the alligator snapping turtle, *Macroclemys temminckii*: *Journal of Thermal Biology*, v. 36, p. 160–166.

Gren, J.A., and Lindgren, J., 2013, Dental histology of mosasaurs and a marine crocodylian from the Campanian (Upper Cretaceous) of southern Sweden: incremental growth lines and dentine formation rates: *Cambridge University Press Geol. Mag*., v. 151, p. 134-143.

Harrell Jr, T.L., Pérez-Huerta, A., and Phillips, G., 2016, Strontium isotope age-dating of fossil shark tooth enameloid from the Upper Cretaceous Strata of Alabama and Mississippi, USA: *Cretaceous Research*, v. 62, p. 1-12.

Harrell Jr, T.L., Pérez-Huerta, A., and Suarez, C.A., 2016, Endothermic Mosasaurs? Possible thermoregulation of Late Cretaceous mosasaurs (Reptilia, Squamata) indicated by stable oxygen isotopes in fossil bioapatite in comparison with coeval marine fish and pelagic seabirds: *Palaeontology*, v. 59, p. 351-363, doi: 10.1111/pala.12240.

Harrell Jr, T.L., and Pérez-Huerta, A., 2015, Habitat preference of mosasaurs indicated by rare earth element (REE) content of fossils from the Upper Cretaceous marine deposits of Alabama, New Jersey, and South Dakota (USA): *Netherlands Journal of Geosciences*, v. 94, p. 145-154

Hays, G.C. and Scott, R., 2013, Global patterns for upper ceilings on migration distance in sea turtles and comparisons with fish, birds and mammals: *Functional Ecology*, v. 27, p. 748-756.

Horton, T.W., Holdaway, R.N., Zerbini, A.N., Hauser, N., Garrigue, C., Andriolo, A., and Clapham, P.J., 2011, Straight as an arrow: humpback whales swim constant course tracks during long-distance migration: *Biology Letters*, v. 7, p. 674-679.

Hückstädt, L.A., Holser, R.R., Tift, M.S., Costa, D.P., 2018, The extra burden of motherhood: reduced dive duration associated with pregnancy status in a deep-diving mammal, the northern elephant seal: *Biology Letters*, v. 14, p. 1-14.

Kermack, K.A., 1956, Tooth Replacement in Mammal-Like Reptiles of the Suborders Gorgonopsia and Therocephalia: *Philosophical Transactions of the Royal Society of London*, v. 240, p. 95–133.

Kohler, N.E., Turner, P.A., Hoey, J.J., Natanson, L.J. and Briggs, R., 2002, Tag and recapture data for three pelagic shark species: BlueShark (Prionace glauca), Shortfin Mako (Isurus xyrinchus), and Porbeagle (Lamna nasus) in the North Atlantic Ocean: *Col.Vol.Sci.Pap. ICCAT*, v.54, no.4, p.1231-1260.

Kohn, M.J., and Cerling, T.E., 2002, Stable Isotope Compositions of Biological Apatite: *Reviews in Mineralogy and Geochemistry*, v. 48, p. 455-488.

Kooyman, G.L., and Castellini, M., 1980, Aerobic and Anaerobic Metabolism During Voluntary Diving in Weddell Seals: Evidence of Preferred Pathways from Blood Chemistry and Behavior: *Journal of Comparative Physiology*, v. 138, p. 335-346.

Lécuyer, C., Amiot, R., Touzeau, A., and Trotter, J., 2013, Calibration of the phosphate $\delta^{18}O$ thermometer with carbonate–water oxygen isotope fractionation equations: *Chemical Geology*, v. 347, p. 217-226.

Lécuyer, C., Picard, S., Garcia, J.P., Sheppard, S. M. F., Grandjean, P. and Dromart, G., 2003, Thermal evolution of Tethyan surface waters during the Middle-Late Jurassic: evidence from $\delta^{18}O$ values of marine fish teeth: *Paleoceanography*, v. 18, p. 1076–1092.

Lillywhite, H.B., Babonis, L.S., Sheehy, III, C.M., and Tu, M.C., 2008, Sea snakes (*Laticauda spp*.) require fresh drinking water: Implication for the distribution and persistence of populations: *Physiol. Biochem. Zool*., v.81, p.785-796.

Lindgren, J., and Siverson, M., 2004, The first record of the mosasaur *Clidastes* from Europe and its palaeogeographical implications: *Acta Palaeontologica Polonica*, v. 49(2), p. 219–234.

Lingham-Soliar, T., 2004, Palaeopathology and injury in the extinct mosasaurs (Lepidosauromorpha, Squamata) and implications for modern reptiles: *Lethaia*, v. 37, p. 255-262.

Liu, K., 2009, Oxygen and carbon isotope analysis of the Mooreville Chalk and late Santonian-early Campanian sea level and sea surface temperature changes, northeastern Gulf of Mexico, U.S.A.: *Cretaceous Research*, v. 30, p. 980-990.

Longinellia, A., 1984, Oxygen isotopes in mammal bone phosphate: A new tool for paleohydrological and paleoclimatological research?: *Geochimica et Cosmochimica Acta*, v. 48, p. 385-390.

Longrich, N.R., Bhullar, B.S., and Gauthier, J.A., 2012, Mass extinction of lizards and snakes at the Cretaceous–Paleogene boundary: *Proceedings of the National Academy of Sciences of the United States of America*, v. 109(52), p. 21396-21401.

Luz, B., Kolodny, Y., and Horowitz, M., 1984, Fractionation of oxygen isotopes between mammalian bone-phosphate and environmental drinking water: *Geochimica et Cosmochimica Acta*, v. 48, p. 1689–1693.

Macleod, N., Rawson, P.F., Forey, P.L., Banner, F.T., Boudagher-Fadel, M.K., Brown, P.R., Burnett, J.A., Chambers, P., Culver, S., Evans, S.E., Jeffery, C., Kaminski, M.A., Lord,

A.R., Milner, A.C., Milner, A.R., Morris, N., Owen, E., Rosen, B.R., Smith, A.B., Taylor, P.D., Urquhart, E., and Young, J.R., 1997, The Cretaceous-Tertiary biotic transition: Journal of the Geological Society, v. 154, p. 265-292.

Madden, P.W., Babcock, M.J., Vayda, M.E., and Cashon, R.E., 2004, Structural and kinetic characterization of myoglobins from eurythermal and stenothermal fish species: *Comparative Biochemistry and Physiology*, v. 137, p. 341–350.

Martin, J.E., Bell, G.L., Jr., Case, J.A., Chaney, D.S., Fernandez, M.S., Gasparini, Z., Reguero, M. and Woodburne, M.O., 2002, Mosasaurs (Reptilia) from the Late Cretaceous of the Antarctic Peninsula, in Gamble, J.A, Skinner, D.N.B. and Henrys, S., Antarctica at the close of a millenium: 8th International Symposium of Antarctic Earth Sciences, Royal Society of New Zealand Bulletin 35, 293-299.

Massare, J.A., 1994, Swimming capabilities of Mesozoic marine reptiles: a review *in* Maddock, L., Bone, Q., and Rayner, J.M.V., The Mechanics and Physiology of Animal Swimming: New York, NY, Cambridge University Press, p. 133-150.

Massare, J.A., 1987, Tooth Morphology and Prey Preference of Mesozoic Marine Reptiles: *Journal of Vertebrate Paleontology*, v. 7(2), p. 121-137.

McKinney, C.R., McCrea, J.M., Epstein, S., Allen, H.A. and Urey, H.A., 1950, Improvements in mass spectrometers for the measurement of small differences in isotope abundance ratios: *Review of Scientific Instruments*, v. 21, p. 724-730.

Newsome, S.D., Clementz, M.T., and Koch, P.L., 2010, Using stable isotope biogeochemistry to study marine mammal ecology: *Marine Mammal Science*, v. 26(3), p. 509-572.

Nicholls, E.L., and Russell, A.P., 1990, Paleobiogeography of the Cretaceous Western Interior Seaway of North America: the vertebrate evidence: *Palaeogeography, Palaeoclimatology, Palaeoecology*, v. 79, p. 149-169.

O'Neil, J.R., Roe, L.J., Reinhard, E., and Blake, R.E., 1994, A rapid and precise method of oxygen isotope analysis of biogenic phosphate: *Israel Journal of Earth Sciences*, v. 43, p. 203-212.

Pagani, M. and Arthur, M.A., 1998, Stable isotopic studies of Cenomanian-Turonian proximal marine fauna from the U.S. Western Interior Seaway: *SEPM Concepts in Sedimentology and Paleontology* v. 6, p. 201-225.

Pellegrini, R.A., 1998, Mosasaur Limb Bone Skeletochronology and Paleohisto-osteology: University of Kansas, 124 p.

Pellegrini, R., 2007, Skeletochronology of the limb elements of mosasaurs (Squamata; Mosasauridae): *Transactions of the Kansas Academy of Science*, v. 110, p. 83-99.

Petersen, S.V., Tabor, C.R., Lohmann, K.C., Poulsen, C.J., Meyer, K.W., Carpenter, S.J., Erickson, J.M., Matsunaga, K.K.S., Smith, S.Y., and Sheldon, N.D., 2016, Temperature and salinity of the Late Cretaceous Western Interior Seaway: *Geology*, v. 44, p. 903-906.

Pucéat, E., Joachimski, M.M., Bouilloux, A., Monna, F., Bonin, A., Motreuil, S., Morinière, P., Hénard, S., Mourin, J., Dera, G., Quesne, D., 2010, Revised phosphate–water fractionation equation reassessing paleotemperatures derived from biogenic apatite: *Earth and Planetary Science Letters*, p. 1-8, doi:10.1016/j.epsl.2010.07.034.

Ross, M.R., 2009, Charting the Late Cretaceous Seas: Mosasaur Richness and Morphological Diversification: *Journal of Vertebrate Paleontology*, v. 29(2), p. 409-416.

Rothschild, B.M., and Martin, L.D., Skeletal Impact of Disease: New Mexico Museum of Natural History and Science, State of New Mexico Department of Cultural Affairs, 2006.

Russell, D.A., Systematics and morphology of American mosasaurs (Reptilia, Sauria), vol. 23: Peabody Museum of Natural History, Yale University, 1967.

Russell, D. A., 1970, The vertebrate fauna of the Selma Formation of Alabama; Part VII, The Mosasaurs: *Fieldiana: Geology Memoirs*, v. 3(7), p. 369-380.

Schulp, A.S., 2005, Feeding the Mechanical Mosasaur: what did Carinodens eat?: *Netherlands Journal of Geosciences*, v. 84, p. 345-357.

Schulp, A.S., Walenkamp, G.H.I.M., Hofman, P.A.M., Rothschild, B.M., Jagt, J.W.M., 2004, Rib Fracture in Prognathodon saturator (Mosasauridae, Late Cretaceous): *Netherlands Journal of Geosciences*, v. 83, p. 251-254.

Sharp, Z.D., 2017, Principles of Stable Isotope Geochemistry 2nd Edition: University of New Mexico, 384 p.

Steuber, T., Rauch, M., Masse, J.P., Graaf, J., and Malkoc, M., 2005, Low-latitude seasonality of Cretaceous temperatures in warm and cold episodes: *Nature*, v. 437, p. 1341-1344.

Straight, W.H., Barrick, R.E., and Eberth, D.A., 2004, Reflections of surface water, seasonality and climate in stable oxygen isotopes from tyrannosaurid tooth enamel: *Palaeogeography, Palaeoclimatology, Palaeoecology*, v. 206, p. 239-256, doi: 10.1016/j.palaeo.2004.01.006.

Standora, E.A., Spotila, J.R., Keinath, J.A., and Shoop, C.R., 1984, Body Temperatures, Diving Cycles, and Movement of a Subadult Leatherback Turtle, *Dermochelys coriacea*: *Herpetologic*, v. 40(2), p. 169-176.

Totten, R., 2009, Oxygen Isotope Evidence for Mosasaur Migration and Fresh Water Incursion [Unpublished Senior Thesis]: University of Kansas, 13 p.

Vennemann, T.W., Fricke, H.C., Blake, R.E., O'Neil, J.R., and Colman, A., 2002, Oxygen isotope analysis of phosphates: a comparison of techniques for analysis of Ag_3PO_4: *Chemical Geology*, v. 185, p. 321-336.

Wang, X., Fan, J.L., Ito, Y., Luan, X., and Diekwisch, T.G.H., 2006, Identification and Characterization of a Squamate Reptilian Amelogenin gene: *Iguana iguana*: *Journal of Experimental Zoology*, v. 306, p. 393-406.

Weir, C.R., 2008, Overt Responses of Humpback Whales (Megaptera novaeangliae), Sperm Whales (Physeter macrocephalus), and Atlantic Spotted Dolphins (Stenella frontalis) to Seismic Exploration off Angola: *Aquatic Mammals*, v. 34(1), p. 71-83.

Woo, K.S., Anderson, T.F., Railsback, L.B., and Sandberg, P.A., 1992, Oxygen Isotope Evidence for High-Salinity Surface Seawater in the Mid- Cretaceous Gulf of Mexico: Implications for Warm, Saline Deepwater Formation: *Paleoceanography*, v. 7(5), p. 673-685.

Yoshida, N., and Miyazaki, N., 1991, Oxygen Isotope Correlation of Cetacean Bone Phosphate With Environmental Water: *Journal of Geophysical Research*, v. 96, p. 815–820.

Zazzo, A., Lécuyer, C., Sheppard, S.M., Grandjean, P. and Mariotti, A., 2004, Diagenesis and the reconstruction of paleoenvironments: a method to restore original δ 18 O values of carbonate and phosphate from fossil tooth enamel: *Geochimica et Cosmochimica Acta*, 68(10), pp.2245-2258.

APPENDIX A. *CLIDASTES* OXYGEN ISOTOPE DATA

Table 1A: Stable Oxygen Isotope Data.

Tooth 3 (Crown to Base)	**$\delta^{18}O$ (‰ V-SMOW)**
T3S40	21.64
T3S39	21.75
T3S38	21.72
T3S37	21.52
T3S36	21.57
T3S35	21.78
T3S34	22.23
T3S33	22.29
T3S32	22.05
T3S31	22.21
T3S30	20.20
T3S29	22.04
T3S28	22.44
T3S27	22.24
T3S26	21.82
T3S25	22.32
T3S23	22.21
T3S22	22.33
T3S21	21.70
T3S20	22.26
T3S19	21.47
T3S18	20.95
T3S17	21.89
T3S16	21.99
T3S15	22.61
T3S14	21.95
T3S13	22.34

T3S12	22.46
T3S11	22.52
T3S10	21.92
T3S9	21.42
T3S8	22.09
T3S7	21.95
T3S6	21.38
T3S5	21.87
T3S4	21.72
T3S3	20.03
T3S2	20.99
T3S1	21.00
Tooth 4 (Crown to Base)	**$\delta^{18}O$ (‰ V-SMOW)**
T4S45	20.59
T4S44	20.83
T4S43	20.55
T4S42	20.31
T4S41	20.95
T4S40	20.43
T4S39	21.36
T4S38	20.79
T4S37	20.05
T4S36	21.11
T4S35	20.86
T4S34	21.24
T4S33	21.05
T4S32	20.30
T4S31	21.16
T4S29	21.55
T4S28	21.15
T4S27	21.39
T4S26	21.13
T4S25	21.00
T4S24	21.25
T4S23	21.47
T4S22	21.47
T4S21	21.45

T4S20	21.42
T4S19	21.70
T4S18	21.17
T4S17	20.66
T4S16	21.59
T4S15	22.45
T4S14	22.47
T4S13	22.00
T4S12	22.57
T4S11	22.18
T4S10	22.32
T4S9	22.16
T4S8	21.93
T4S7	21.91
T4S6	22.52
T4S5	22.59
T4S4	22.17
T4S3	21.94
T4S2	22.00
T4S1	22.00
Tooth 5 (Crown to Base)	**$\delta^{18}O$ (‰ V-SMOW)**
T5S52	20.53
T5S51	20.78
T5S50	20.83
T5S49	20.85
T5S48	20.85
T5S47	20.99
T5S46	21.12
T5S45	21.59
T5S44	21.00
T5S43	21.23
T5S42	20.83
T5S41	21.08
T5S40	21.16
T5S39	21.54
T5S38	20.99
T5S37	21.37

T5S36	21.26
T5S35	21.23
T5S34	21.25
T5S33	21.40
T5S32	21.34
T5S31	21.67
T5S30	21.63
T5S29	21.93
T5S28	21.37
T5S27	21.58
T5S26	21.50
T5S25	21.67
T5S24	21.72
T5S23	21.94
T5S22	21.62
T5S21	19.54
T5S20	21.70
T5S19	21.62
T5S18	22.03
T5S17	21.85
T5S16	21.66
T5S15	21.91
T5S14	20.05
T5S13	21.91
T5S12	21.88
T5S11	21.93
T5S10	22.45
T5S9	21.80
T5S8	22.36
T5S7	22.28
T5S6	21.88
T5S5	21.96
T5S4	21.94
T5S3	21.84
T5S2	22.06
T5S1	21.55
Tooth 6 (Crown to Base)	**$\delta^{18}O$ (‰ V-SMOW)**

T6S56	19.45
T6S51	18.82
T6S49	18.41
T6S48	19.36
T6S46	18.96
T6S45	18.42
T6S44	19.15
T6S43	19.09
T6S42	19.46
T6S40	19.86
T6S39	19.06
T6S38	19.86
T6S37	20.29
T6S36	20.78
T6S35	20.87
T6S34	20.61
T6S33	21.14
T6S32	21.05
T6S31	22.13
T6S30	21.15
T6S29	20.61
T6S28	20.61
T6S27	20.53
T6S25	20.78
T6S15	19.70
T6S14	20.55
T6S9	19.57
T6S8	21.32
T6S7	16.96
T6S6	20.46
T6S5	20.65
T6S4	21.32
T6S3	20.04
T6S2	19.99
T6S1	20.46
Tooth 7 (Crown to Base)	**$\delta^{18}O$ (‰ V-SMOW)**
T7S50	19.94

T7S49	21.70
T7S21	22.84
T7S20	23.14
T7S18	21.99
T7S17	22.33
T7S16	22.04
T7S15	22.28
T7S12	22.29
T7S11	22.24
T7S10	21.42
T7S9	21.37
T7S8	21.35
T7S7	21.79
T7S6	21.85
T7S5	22.58
T7S3	21.84
T7S2	21.99
T7S1	21.68
Tooth 8 (Crown to Base)	**$\delta^{18}O$ (‰ V-SMOW)**
T8S43	20.42
T8S42	20.27
T8S41	20.46
T8S40	20.22
T8S39	20.49
T8S38	20.39
T8S37	19.58
T8S36	20.53
T8S35	20.12
T8S34	20.74
T8S33	20.16
T8S32	19.90
T8S30	20.21
T8S29	20.32
T8S28	20.07
T8S27	20.27
T8S26	20.05
T8S25	20.18
T8S24	20.56
T8S23	20.16

T8S22	20.00
T8S21	20.47
T8S20	20.48
T8S19	20.30
T8S18	20.42
T8S17	20.75
T8S16	20.70
T8S15	20.62
T8S14	22.02
T8S13	22.15
T8S12	21.10
T8S11	21.13
T8S10	21.22
T8S9	21.33
T8S8	21.15
T8S7	21.42
T8S6	21.75
T8S5	21.36
T8S4	20.75
T8S3	18.56
T8S1	21.76
Tooth 11 (Crown to Base)	**$\delta^{18}O$ (‰ V-SMOW)**
T11S41	20.47
T11S40	20.13
T11S39	20.34
T11S38	20.36
T11S37	20.24
T11S36	20.04
T11S35	20.69
T11S34	20.29
T11S33	20.40
T11S32	20.30
T11S31	20.34
T11S30	20.01
T11S29	19.85
T11S28	19.71
T11S27	19.47
T11S26	20.33
T11S25	19.76

T11S24	20.30
T11S23	19.29
T11S22	19.72
T11S21	19.21
T11S20	19.39
T11S19	19.42
T11S18	20.14
T11S17	20.00
T11S16	19.96
T11S15	19.56
T11S14	19.40
T11S13	20.00
T11S12	20.37
T11S11	20.17
T11S10	19.96
T11S9	19.94
T11S8	20.06
T11S7	20.13
T11S6	20.76
T11S5	19.27
T11S4	21.67
T11S3	20.73
T11S2	20.36
T11S1	21.17
Tooth 13 (Crown to Base)	**$\delta^{18}O$ (‰ V-SMOW)**
T13S48	21.65
T13S47	20.24
T13S46	19.94
T13S45	20.38
T13S44	20.17
T13S43	20.26
T13S42	19.16
T13S41	19.93
T13S40	19.51
T13S38	19.44
T13S37	19.51
T13S36	20.00
T13S35	19.58
T13S34	19.92

T13S33	19.50
T13S32	20.38
T13S31	20.58
T13S30	19.45
T13S29	19.08
T13S28	19.56
T13S27	19.07
T13S25	19.26
T13S24	19.24
T13S23	20.09
T13S22	20.41
T13S21	19.65
T13S20	19.79
T13S19	20.33
T13S18	19.57
T13S17	19.65
T13S16	20.07
T13S15	19.65
T13S14	19.43
T13S13	19.57
T13S12	19.26
T13S11	19.39
T13S10	19.63
T13S9	18.89
T13S8	20.08
T13S7	19.56
T13S6	19.01
T13S5	19.45
T13S4	19.84
T13S3	19.78
T13S2	19.62
T13S1	17.97

Figures 1-7A: Growth line analysis for each tooth

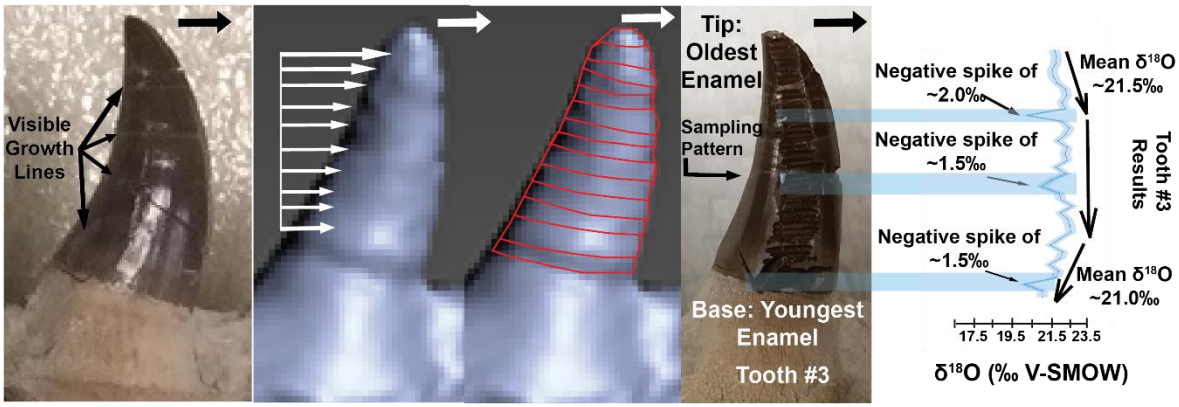

Figure 1A: Visible external growth lines of the *C. propython* Tooth #3, from a white light photo (a) and 3D scan before sampling (b, c) and after (d). Oxygen isotope results are plotted alongside the tooth (e), with negative excursions highlighted.

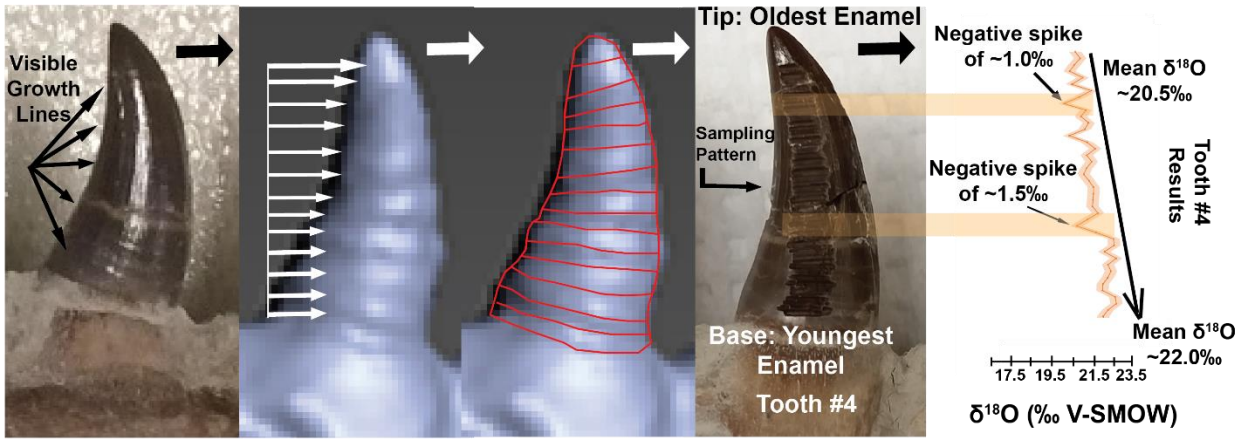

Figure 2A: Visible external growth lines of the *C. propython* Tooth #4, from a white light photo (a) and 3D scan before sampling (b, c) and after (d). Oxygen isotope results are plotted alongside the tooth (e), with negative excursions highlighted.

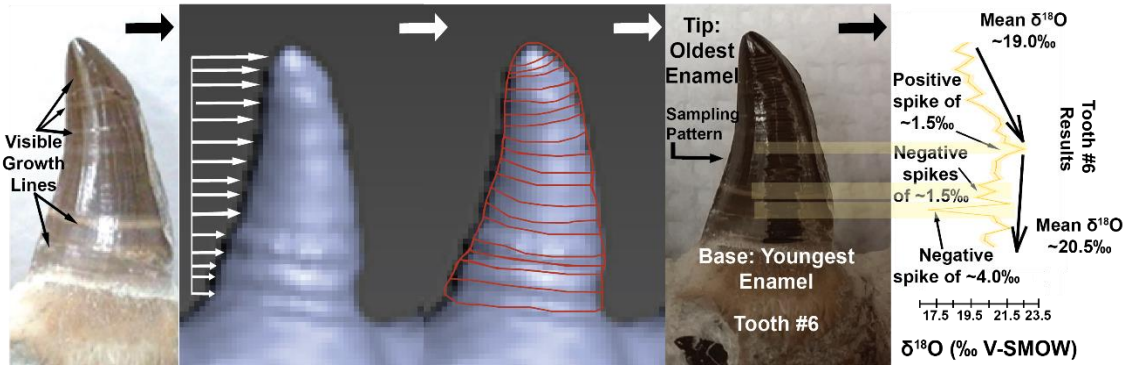

Figure 3A: Visible external growth lines of the *C. propython* Tooth #6, from a white light photo (a) and 3D scan before sampling (b, c) and after (d). Oxygen isotope results are plotted alongside the tooth (e), with negative and positive excursions highlighted.

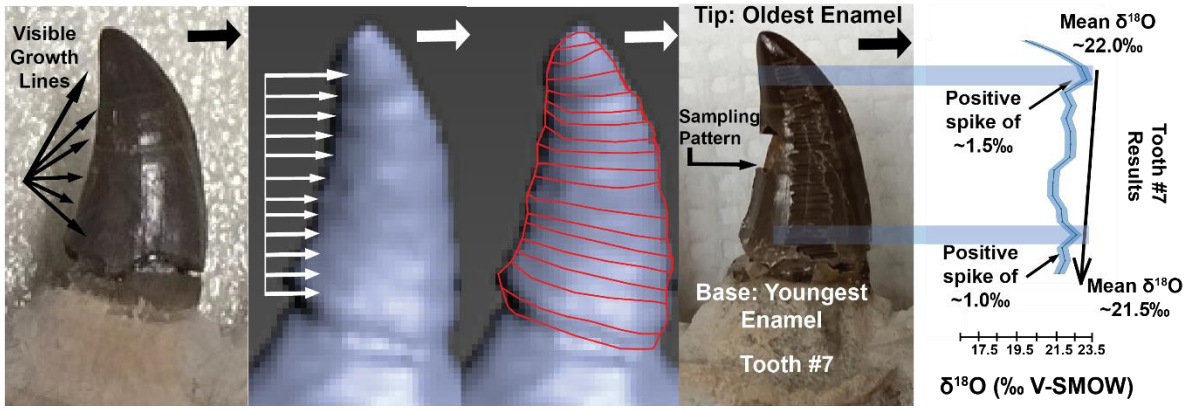

Figure 4A: Visible external growth lines of the *C. propython* Tooth #7, from a white light photo (a) and 3D scan before sampling (b, c) and after (d). Oxygen isotope results are plotted alongside the tooth (e), with positive excursions highlighted.

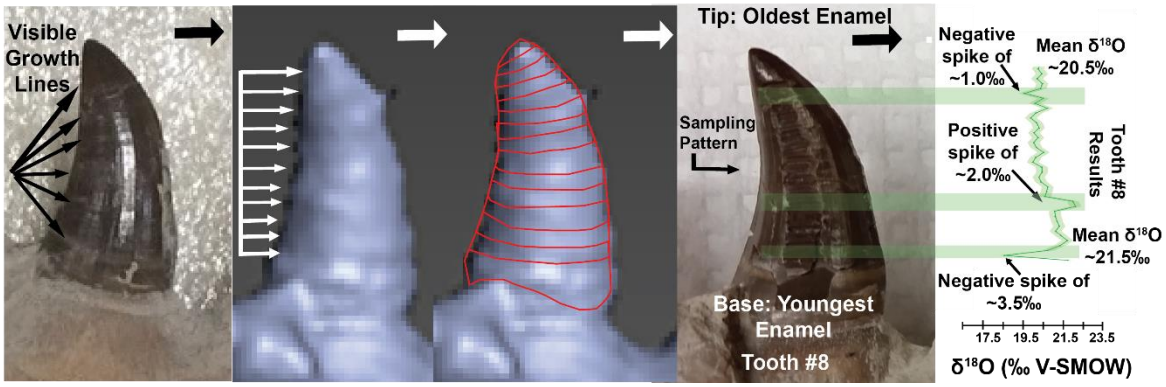

Figure 5A: Visible external growth lines of the *C. propython* Tooth #8, from a white light photo (a) and 3D scan before sampling (b, c) and after (d). Oxygen isotope results are plotted alongside the tooth (e), with negative and positive excursions highlighted.

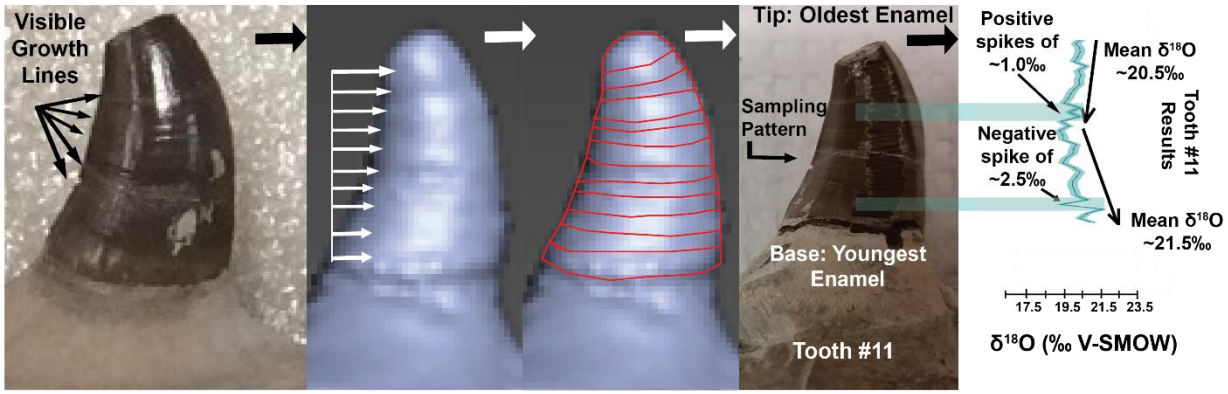

Figure 6A: Visible external growth lines of the *C. propython* Tooth #11, from a white light photo (a) and 3D scan before sampling (b, c) and after (d). Oxygen isotope results are plotted alongside the tooth (e), with negative and positive excursions highlighted.

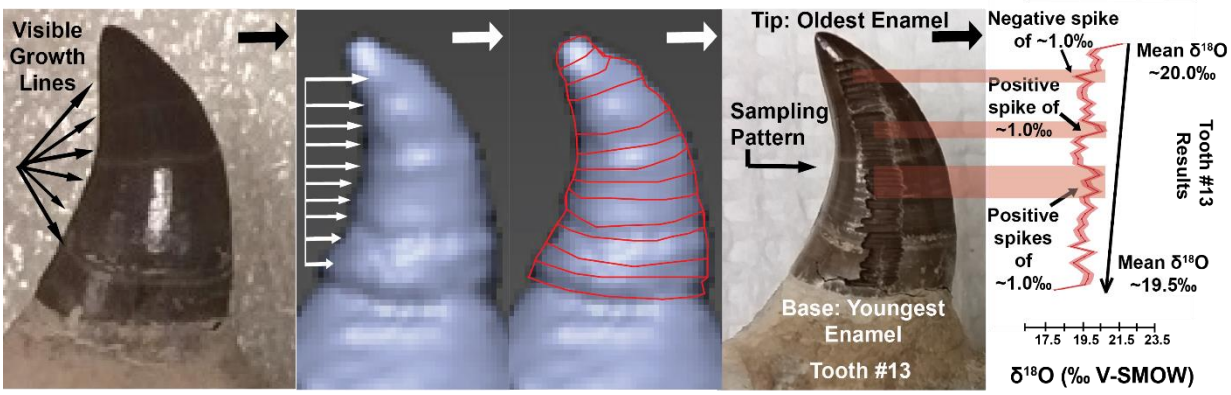

Figure 7A: Visible external growth lines of the *C. propython* Tooth #13, from a white light photo (a) and 3D scan before sampling (b, c) and after (d). Oxygen isotope results are plotted alongside the tooth (e), with negative and positive excursions highlighted.

APPENDIX B. GROWTH LINE COUNTS AND TEMPERATURE CALCULATIONS

Table 1B: Superficial growth line counts.

Tooth #	von Ebner line counts	Andresen line counts	Total estimated days
3	64	2	86
4	67	2	89
5	74	2	96
6	76	2	98
7	75	2	97
8	80	2	102
11	53	3	86
13	48	4	92

Table 2B: Temperature Calculations.

Temperature calculations were performed using the formula for biogenic apatite outlined in Pucéat et al., 2010:

$$\mathbf{T(°C) = 118.7–4.22[(\delta^{18}O_p + (22.6 - \delta^{18}O_{NBS120c})) - \delta^{18}O_w]}$$

To estimate whether seasonality is responsible for the gradual changes in $\delta^{18}O$, temperature was calculated for the mean low values of $\delta^{18}O$ and the mean high values of $\delta^{18}O$ in the combined record. The calculations were then compared and the resulting temperature difference was determined. The hypothesized $\delta^{18}O_w$ of the Late Cretaceous ocean is estimated to have been between 0.0‰ and 1.0‰ (Lécuyer et al., 2003). Here I take the value of 0.0‰ for $\delta^{18}O_w$, as the shallow waters and warmer temperatures of the ME would have caused increased evaportation and thus enriched the water in ^{18}O, and turtle bone $\delta^{18}O_w$ calculations on ME specimens from Alabama further support a value closer to 0.0‰ (Harrell et al., 2016).

	$\delta^{18}O$ Value	**Calculated Temperature (°C)**	**Temperature Difference**
Mean high value of $\delta^{18}O$	22.5‰	23.8 °C	13.9°C
Mean low value of $\delta^{18}O$	19.2‰	37.7 °C	

Table 3B: Body Temperature Calculations.

Body temperature calculations were performed using the formula for biogenic apatite outlined in Lécuyer, 2013:

$$\mathbf{T_{body}(°C) = 117.4–4.5(\delta^{18}O_p - \delta^{18}O_{bodywater})}$$

Averaging the values of the negative excursion amplitudes provided ~3.0‰ as the mean $\delta^{18}O$ excursion amplitude. Body temperature was calculated for the mosasaur body during average

values (*Clidastes* overall mean $\delta^{18}O$ of 20.8‰) versus during an excursion (~3.0‰ mean excursion amplitude subtracted from *Clidastes* overall mean $\delta^{18}O$ of 20.8‰). In fully marine organisms incapable of travelling onto land, $\delta^{18}O_{bodywater}$ of the organism should be equivalent to $\delta^{18}O_{seawater}$ (Newsome et al., 2010; Koch 2007; Clementz and Koch, 2001). Although there are no precise modern analogues for mosasaurs, they were aquatic-bound swimming lizards, therefore modern fully marine organisms incapable of traveling on land may provide the best comparison. Studies on modern fully marine organisms, such as cetaceans and pinnipeds, indicate that they have a body water isotopic ratio comparable to the isotopic ratio of the water the organism is inhabiting (Clementz and Koch, 2001; Yoshida and Miyazaki, 1991). Therefore, here I take the value of 0.0‰ for $\delta^{18}O_{bodywater}$, as it is in equilibrium with $\delta^{18}O_{seawater}$.

	$\delta^{18}O$ Value	**Calculated Temperature (°C)**	**Temperature Difference**
Mean value of $\delta^{18}O$ for *Clidastes*	20.8‰	23.8 °C	13.2°C
Mean value of $\delta^{18}O$ during an excusion	17.8‰	37.0 °C	

APPENDIX C. SPLICING PROCEDURE

Table 1C: Splicing Calculations.

To correlate the records, the alternate mode of tooth replacement was employed to determine an offset pattern when aligning each isotope record. Correlation using this mode was attempted using both a front-to-back (anterior to posterior) and back-to-front (posterior to anterior) replacement wave (Figs. 1C and 2C). When correlation using this mode was not achievable, the sequential mode of tooth replacement was attempted and the front-to-back and the back-to-front replacement waves were plotted (Figs. 3C and 4C). Correlation was successfully achieved using the sequential mode of tooth replacement with a back-to-front replacement wave (Fig. 4C).

In addition to the pattern of tooth replacement, the numerical lag in development between one tooth to the next needed to be estimated. To calculate the numerical amount of offset, modern organisms were utilized as analogues. Unfortunately numerical tooth replacement pattern studies on the nearest living relatives of mosasaurs (komodo dragons and snakes) are lacking; however, numerical tooth replacement calculations were performed on a skink from the order Squamata. This study determined that when comparing the size of successive replacement teeth in a skink, each replacement tooth is preceded by a replacement tooth approximately 20% less developed (Delgado et al., 2003). Taking this model, calculations were performed to estimate 20% of each tooth (Table 1C; Fig. 5C). Next, the records were compiled using the calculated lag and replacement wave patterns (Fig. 5C). It is important to note that once this had been performed not only did an overall trend correlate, but all negative excursions in the tooth

records independently correlated, lending confidence that the negative excursions are real indicators of changing water isotopic composition and not the product of sampling artifacts. After compilation, the correlated record was further aligned to account for missing samples in Tooth #6 and Tooth #7, as well as any suspected sample aliasing (Fig. 6C). During this final correlation process, all previously correlated negative excursions, positive excursions, and the overall secular trend were kept constant.

Tooth #	**Total Length**	**20% of the length**	**Corresponding sample number**
Tooth 3	22 mm	4.4 mm	Sample #8 (T3S33)
Tooth 4	23 mm	4.6 mm	Sample #9 (T4S37)
Tooth 5	25 mm	5 mm	Sample #10 (T5S42)
Tooth 6	26 mm	5.2 mm	Sample #11 (T6S39)
Tooth 7	28 mm	5.6 mm	Sample #10 (T7S40)
Tooth 8	27 mm	5.4 mm	Sample #9 (T8S34)
Tooth 11	21 mm	4.2 mm	Sample #8 (T11S33)
Tooth 13	20 mm	4 mm	Sample #9 (T13S38)

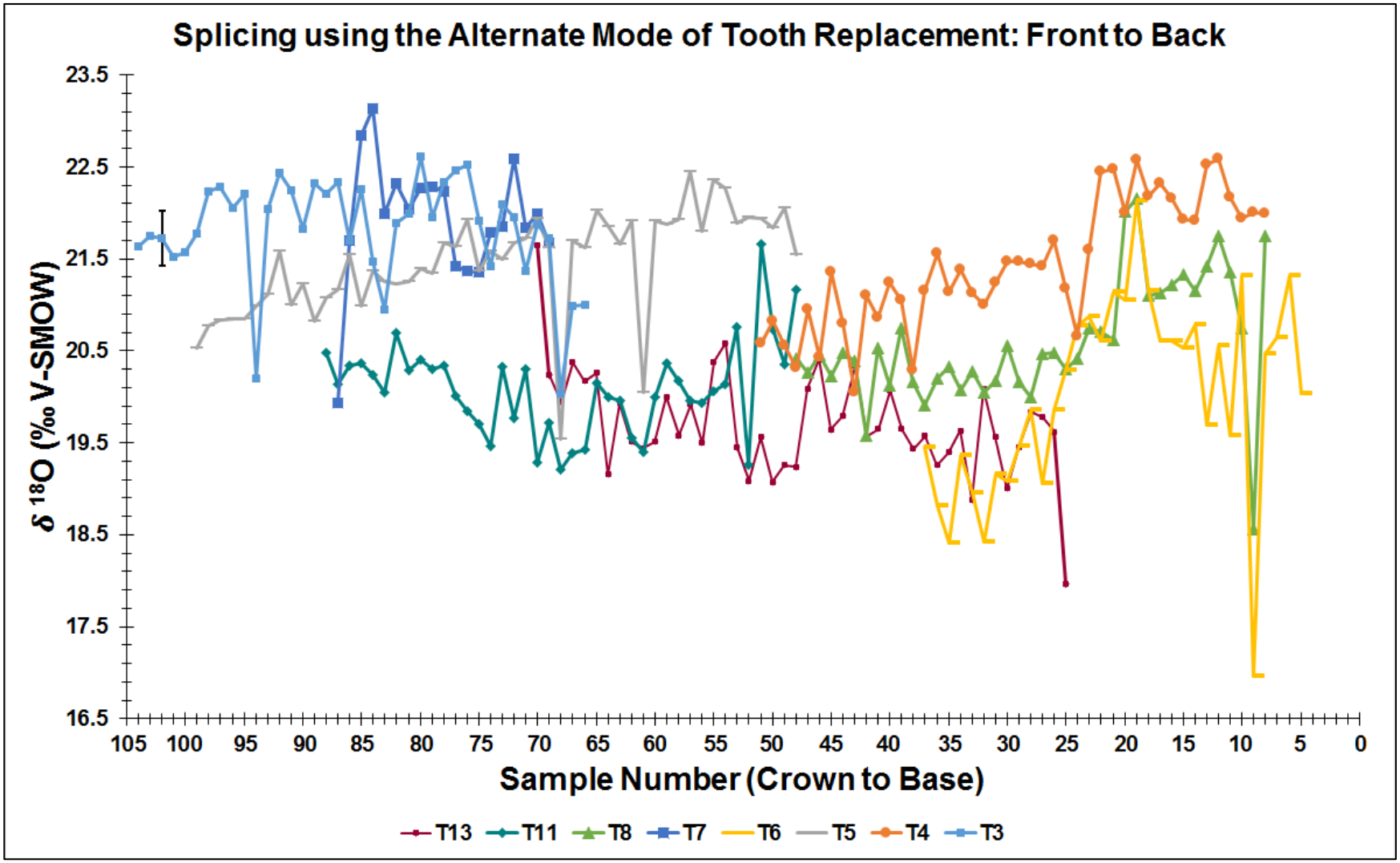

Figure 1C: Splicing using the alternate mode of tooth replacement and a front-to-back replacement wave. Analytical precision is represented on data point #3 of tooth #3.

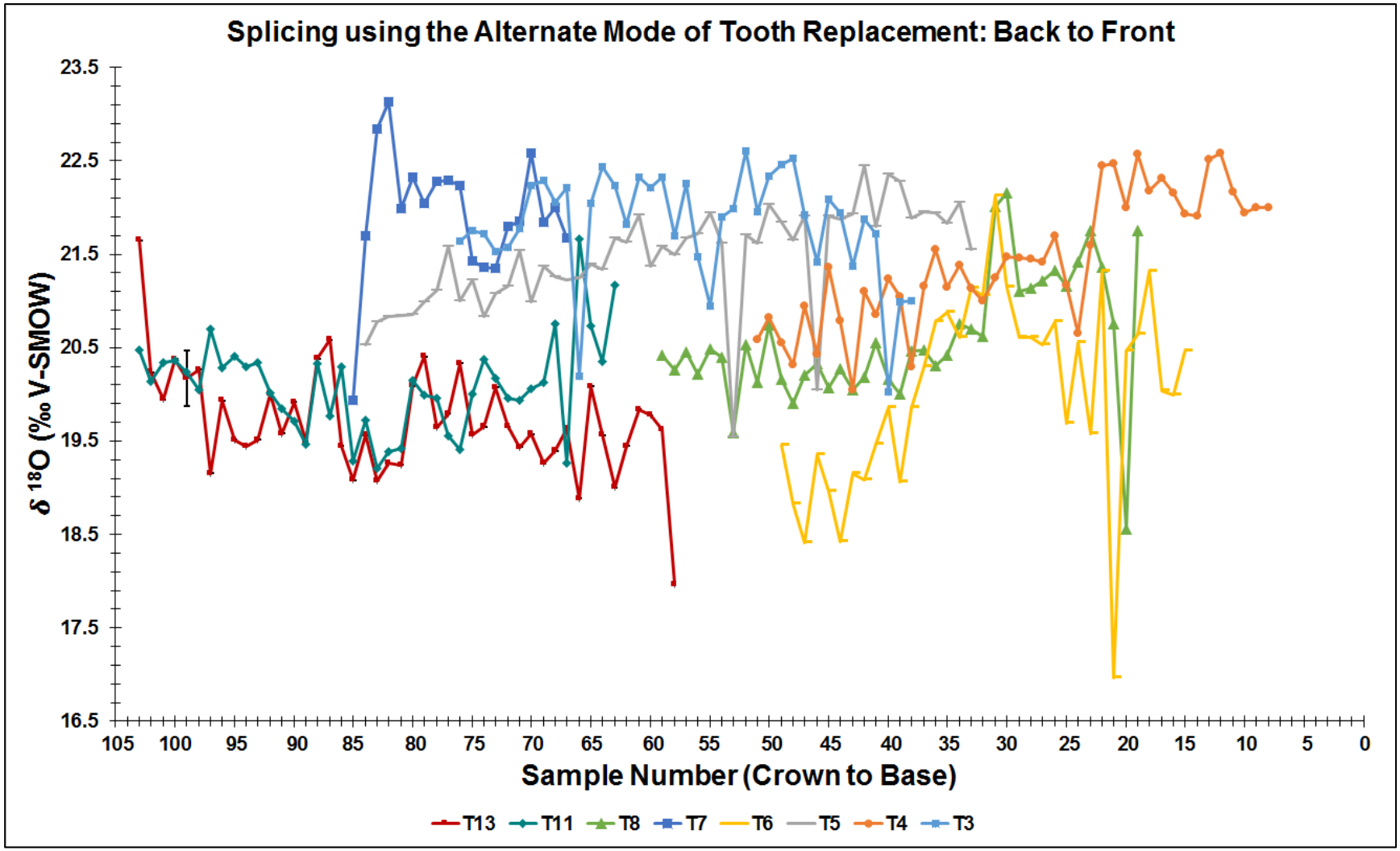

Figure 2C: Splicing using the alternate mode of tooth replacement and a back-to-front replacement wave. Analytical precision is represented on data point #5 of tooth #13.

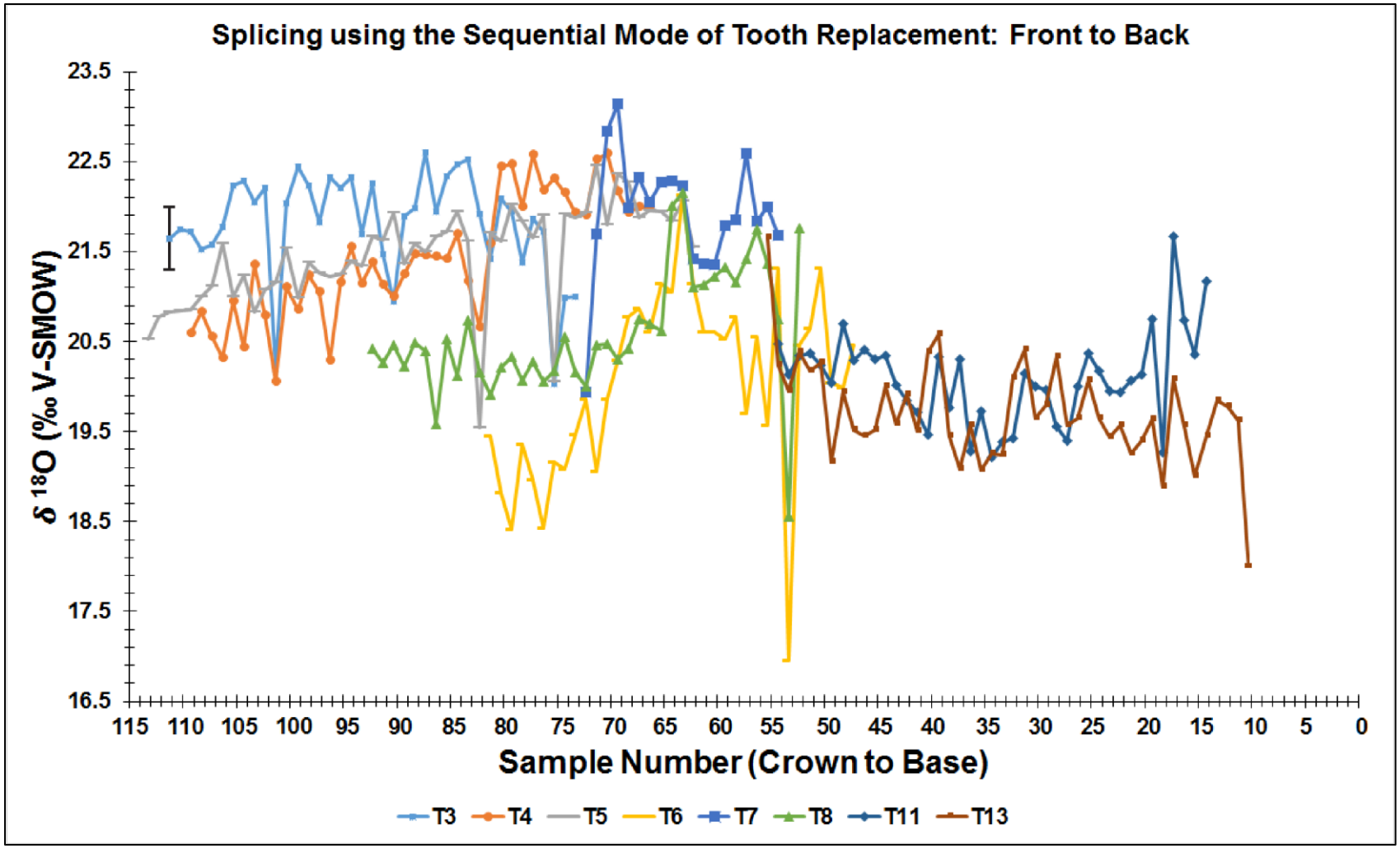

Figure 3C: Splicing using the sequential mode of tooth replacement and a front-to-back replacement wave. Analytical precision is represented on data point #1 of tooth #3.

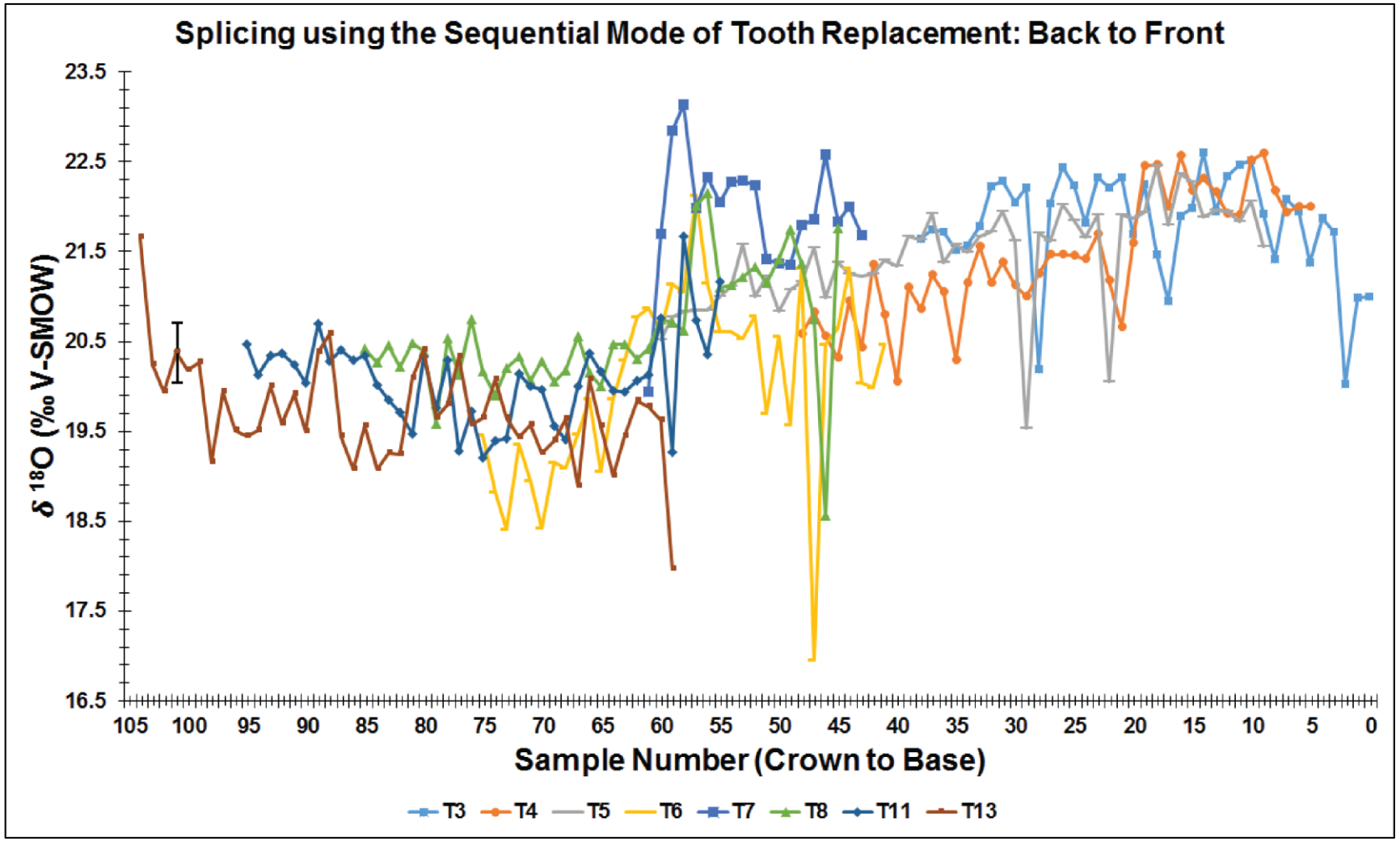

Figure 4C: Splicing using the sequential mode of tooth replacement and a back-to-front replacement wave. Analytical precision is represented on data point #4 of tooth #13.

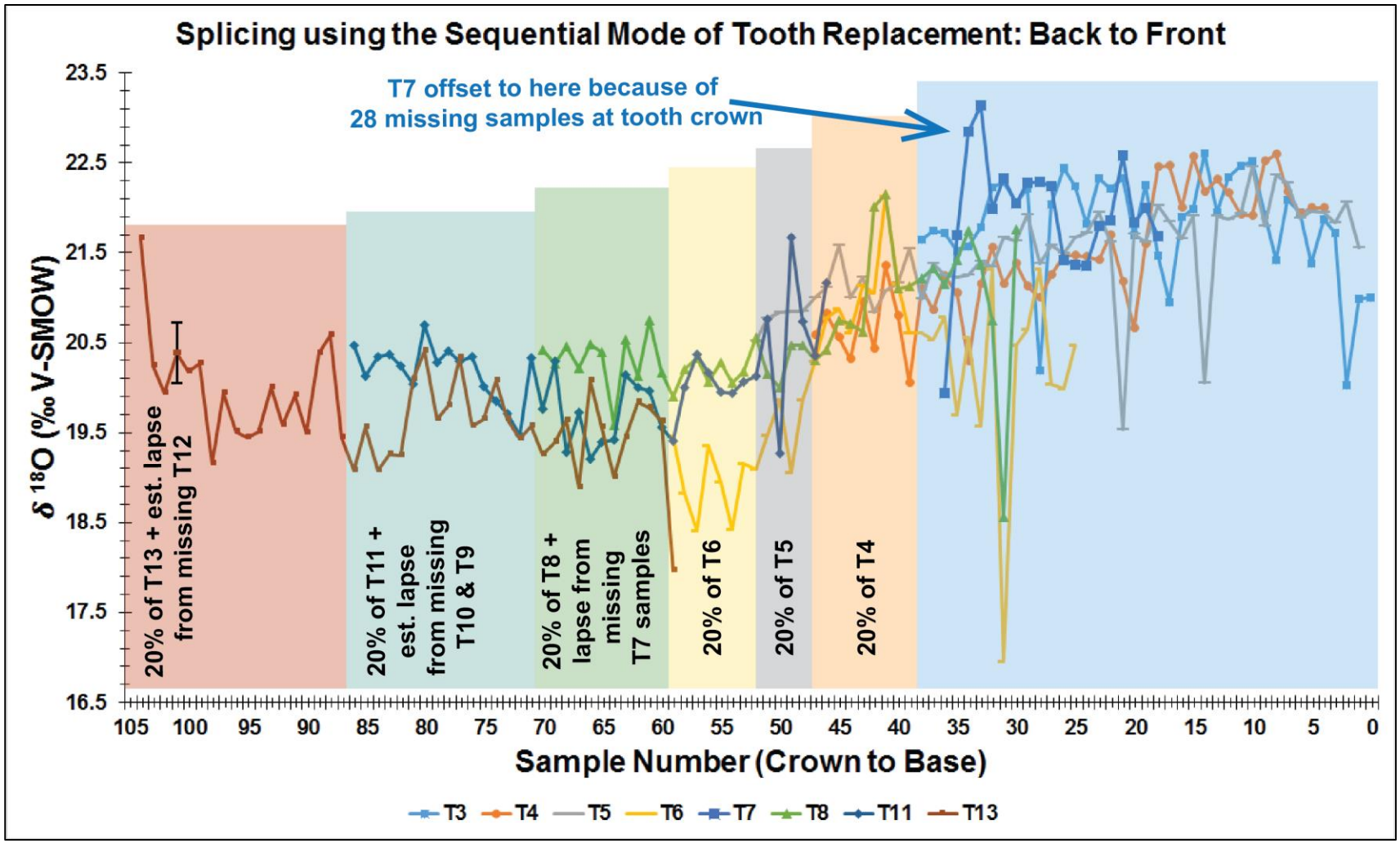

Figure 5C: Tooth records correlated using the 20% development lag calculations and sequential tooth replacement mode in a back-to-front replacement wave. Analytical precision is represented on data point #4 of tooth #13.

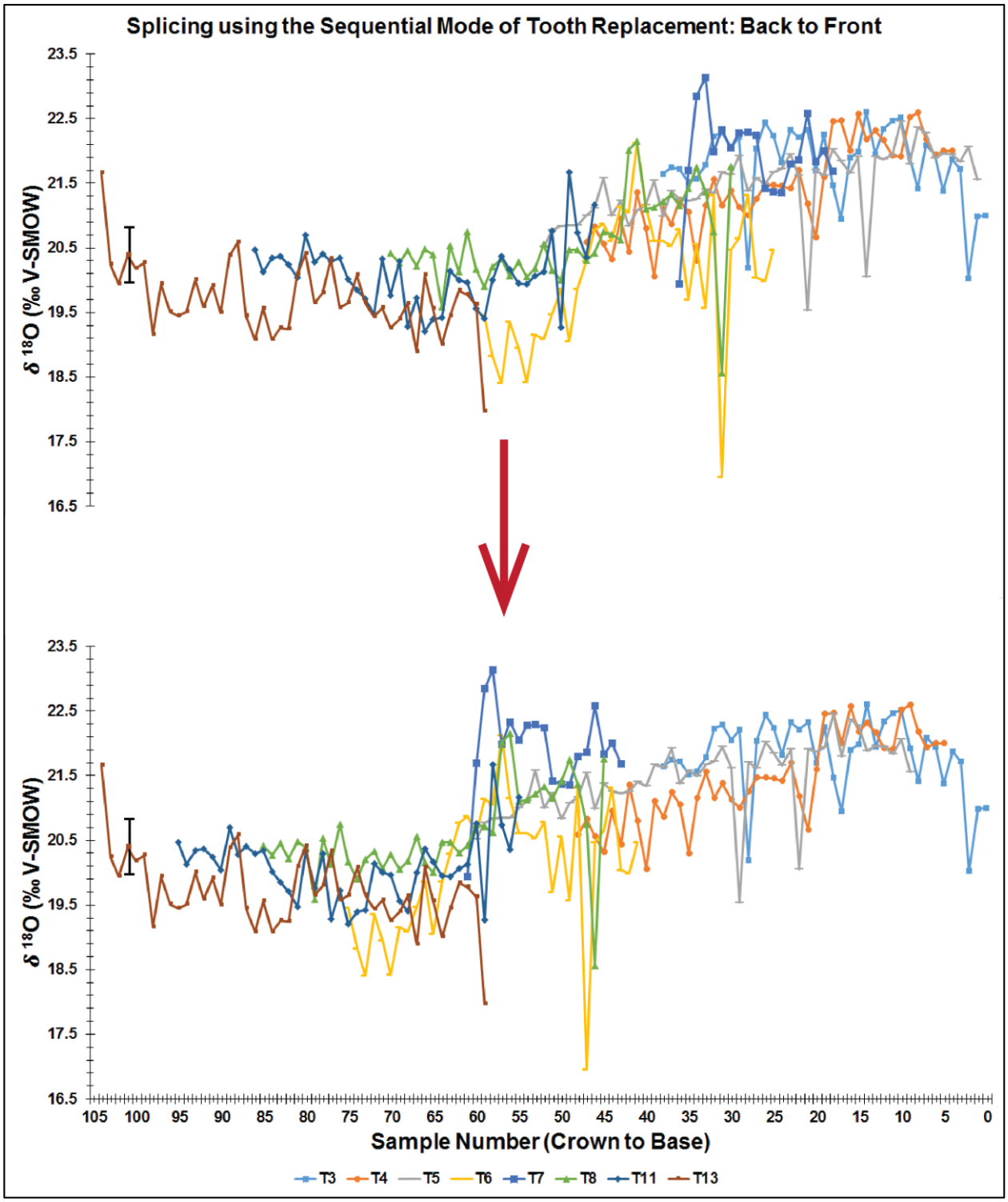

Figure 6C: Final correlation of compiled records to further offset for missing samples in Tooth #6 and #7 and to account for any suspected sample aliasing. Analytical precision is represented on both graphs on data point #4 of tooth #13.